Journal of Drug Delivery Science and Technology 114 (2025) 107435

Contents lists available at ScienceDirect

Journal of Drug Delivery Science and Technology

journal homepage: www.elsevier.com/locate/jddst

Review Article

A critical review of advances and challenges in microinjection moulding of polymeric microneedles

Pouria Azarikhah [a,b], Asim Mushtaq [b], Khaled Mohammed Saifullah [a,c], Philip D. Prewett [d,e], Graham J. Davies [f,g], Zahra Faraji Rad [h,*]

[a] School of Engineering, University of Southern Queensland, Queensland, 4300, Australia
[b] Centre for Future Materials, Institute for Advanced Engineering and Space Sciences, University of Southern Queensland, Queensland, Australia
[c] Hazelton Technologies Pty Ltd, Wynnum, Queensland, 4178, Australia
[d] Department of Mechanical Engineering, University of Birmingham, Birmingham, B15 2TT, United Kingdom
[e] Oxacus Ltd, Dorchester-on-Thames, OX10 7HN, United Kingdom
[f] Faculty of Engineering, UNSW Australia, NSW, 2052, Australia
[g] College of Engineering & Physical Sciences, School of Engineering, University of Birmingham, Birmingham, B15 2TT, United Kingdom
[h] School of Science, Technology and Engineering, University of the Sunshine Coast, Petrie, Queensland, Australia

ARTICLE INFO

Keywords:
Microneedles
Thermoplastic polymers
Microinjection moulding
Negative metal mould
Laser micromachining

ABSTRACT

Microneedles are an innovative alternative to hypodermic needles for delivering vaccines and therapeutic agents and sampling biofluids for point-of-care diagnostics. Two key advantages of microneedle patches over hypodermic needles are their painless application and ease of use without requiring skilled personnel. Polymers stand out as an ideal material for the mass production of microneedles, offering a combination of low cost, good mechanical properties, biocompatibility, biodegradability, and high chemical stability. Among different polymer fabrication techniques, microinjection moulding is a well-established industrial process with high potential to address the challenge of mass-producing microneedle devices cost-effectively and efficiently. Despite the significant potential of the technique, research in this area is limited. This article comprehensively reviews the recent advancement in the fabrication of polymeric microneedles via microinjection moulding. It covers injection moulding steps, mould fabrication, and quality assessment of the final product, with a focus on the challenges associated with the mass manufacturing of microneedles. The article investigates the laser micromachining process and its challenges in fabricating negative metal moulds for microneedles, elaborating on the critical role of mould manufacturing in precisely shaping mould-injected microneedles. The physical and rheological properties of thermoplastic polymers that affect the quality of mould-injected microneedles are also reviewed. Finally, opportunities and future directions for advancing research in this field are discussed.

1. Introduction

For decades, various techniques have been utilised to administer medicines into the human body for medical treatment, including oral, parenteral, inhalation, and transdermal routes. The oral pathway is the most convenient method for patients; however, long-term use can pose limitations due to potential organ toxicity. Additionally, delivering some drugs via the oral route is not feasible due to poor absorption and drug degradation in some body organs such as the liver, kidney, and gastrointestinal tract [1,2]. Conventional injection methods, such as hypodermic needle injections, offer rapid and direct drug delivery. However, it is usually associated with needle anxiety and pain [3].

Transdermal drug delivery (TDD) involves administering therapeutic agents through the skin. This method addresses many limitations of oral drug delivery and allows for more controlled medication release over time [4]. The large surface area of the skin makes it an accessible pathway for drug delivery [5]. Structurally, the skin consists of three layers: the epidermis, dermis, and hypodermis. The outermost part of the epidermis, known as the stratum corneum (SC), serves as the skin's primary protective layer [6].

Microneedles, as TDD systems, offer a promising alternative to improve patient compliance and safety by minimising pain and anxiety associated with hypodermic injections [7,8]. These micron-sized needles present advantages such as sustained release, low logistic expenses,

* Corresponding author. School of Science, Technology and Engineering, University of the Sunshine Coast, Petrie, Queensland, Australia.
E-mail address: zfarajirad@usc.edu.au (Z. Faraji Rad).

https://doi.org/10.1016/j.jddst.2025.107435
Received 19 January 2025; Received in revised form 19 August 2025; Accepted 20 August 2025
Available online 20 August 2025

ease of use, feasibility of self-administration, easy disposal, and the potential for vaccination in rural and remote areas [1,9,10]. In addition to substance delivery, diagnostic microneedles have the potential to be applied minimally invasive to the skin for the collection of interstitial fluid (ISF), which contains distinct biomarkers useful for disease diagnostics [11–14]. Fig. 1 compares the penetration depth of TDD systems, such as microneedle and topical patches, and topical cream with conventional hypodermic needles.

Microneedles are classified into solid, coated, dissolving, hydrogel-forming (HF), and hollow types, as shown in Fig. 2. Solid and hollow polymeric microneedles can be fabricated using the microinjection moulding [16,17]. The "poke and patch" strategy is related to solid microneedles and involves two steps: skin puncture followed by the application of a drug solution to the skin (Fig. 2a) [18]. A key advantage of solid microneedles is the wide range of materials, such as thermoplastic polymers, that can be used in various fabrication techniques, including microinjection moulding [19,20]. Hollow microneedles use a "poke and flow" strategy, in which fluid is injected via internal bores of the needles (Fig. 2e). Microinjection moulding of polymeric hollow microneedles is challenging due to difficulties in negative mould fabrication, the need for post-processing to create fluidic channels, or the requirement for alternative techniques such as investment casting [17,21,22]. This type of microneedle must be manufactured with robust materials to resist breakage due to internal fluid pressure [23].

Polymeric microneedles fabricated using injection moulding have been explored for TDD applications, either through surface drug coating using solid microneedles or by delivering drug through the micro-holes of hollow microneedles [24,25]. Park et al. [26] demonstrated the potential of mould-injected microneedles for delivering a wide range of drugs. Zhang et al. [27] studied coated microneedles with an aqueous lidocaine solution for rapid administration within 1 min. The study was further developed by incorporating clonidine as an adjuvant in the lidocaine formulation, which significantly influenced the coating quality and dissolution behaviour of the drug-loaded layers [28]. Additionally, plasma treatment was applied to enhance drug adsorption and improve the release profile from mould-injected microneedles, thereby improving TDD [29].

Polymeric materials are emerging as an ideal candidate for the mass production of microneedles. Their advantages, including low cost, acceptable mechanical properties, biocompatibility, biodegradability, and high chemical stability, make them a favourable candidate for the mass production of microneedles. Accordingly, polymeric micro-scale needle fabrication has increased widely in recent studies [30].

Factors such as manufacturing time, cost, application, and, consequently, the possibility of mass production define the type of fabrication methods. The most significant challenge of microneedle fabrication is finding an inexpensive and time-efficient technique with the minimum possible complexity to produce microneedles. Among all manufacturing techniques, there is a great potential for mass production of polymeric microneedles by microinjection moulding compared to all other methods [31]. However, despite its great potential, the technique has received limited interest. Fig. 3 shows the number of research papers published since 2005 on the microinjection moulding technique versus all other methods used to fabricate polymeric microneedles, along with the percentage of publications on microinjection moulding compared to all fabrication techniques for each year. The analysis shows that 411 articles, excluding review papers, are related to all manufacturing techniques. In contrast, only 32 research papers were identified with keywords including injection moulding, microneedle, and fabrication or manufacturing. Although microinjection moulding has received less attention than other methods in recent years, its potential for mass production of polymeric microneedles is evident.

This technology-oriented review paper investigates micro-scale injection moulding techniques and negative mould fabrication methods for the manufacturing of polymeric microneedles. To the authors' knowledge, this is the first comprehensive review paper on microinjection moulding for manufacturing microneedles. The study aims to fill the knowledge gap by investigating and reviewing recent developments in the field, mainly analysing the process steps, equipment requirements, injection moulding characteristics, mould manufacturing, quality assessment in mass production, and associated challenges that have not been thoroughly explored previously. In addition, the feasibility of mass production of microneedles using injection moulding is discussed.

2. Polymeric materials for fabrication of microneedles

Polymeric microneedles have been widely used in recent years to overcome obstacles related to the fabrication of microneedles with other materials [33]. Various kinds of biodegradable polymers, including polyvinyl alcohol (PVA), polyvinylpyrrolidone (PVP), polycarbonate (PC), polypropylene (PP), poly methyl methacrylate (PMMA), polylactic

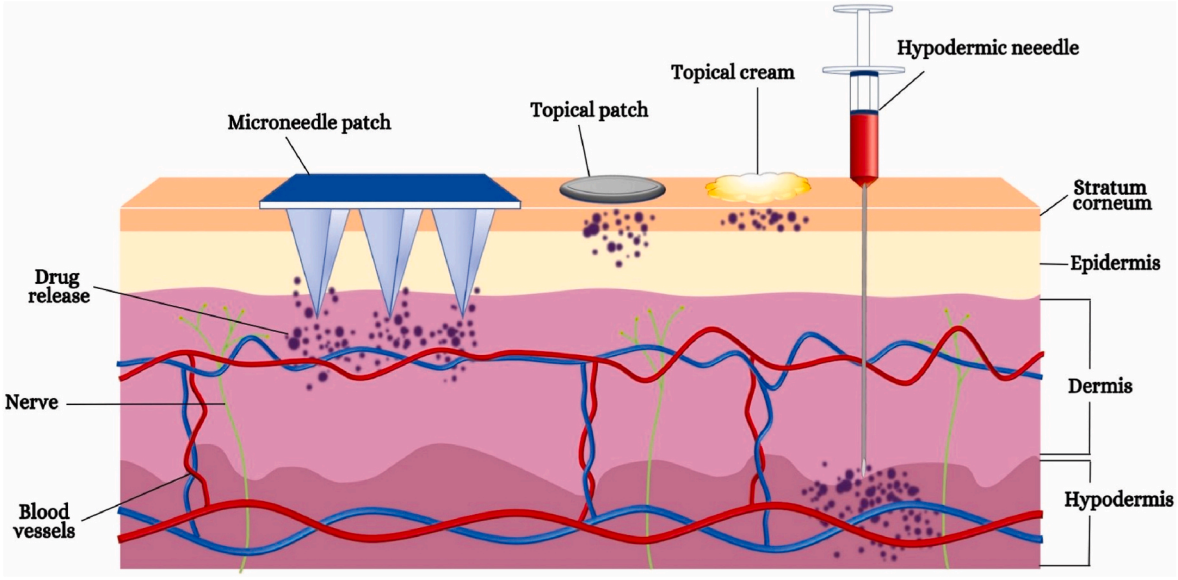

Fig. 1. Comparison of penetration depth of TDD systems, including microneedle patch, topical patch, and topical cream with hypodermic needles. Reproduced with permission from Ref. [15], Copyright 2024, Elsevier.

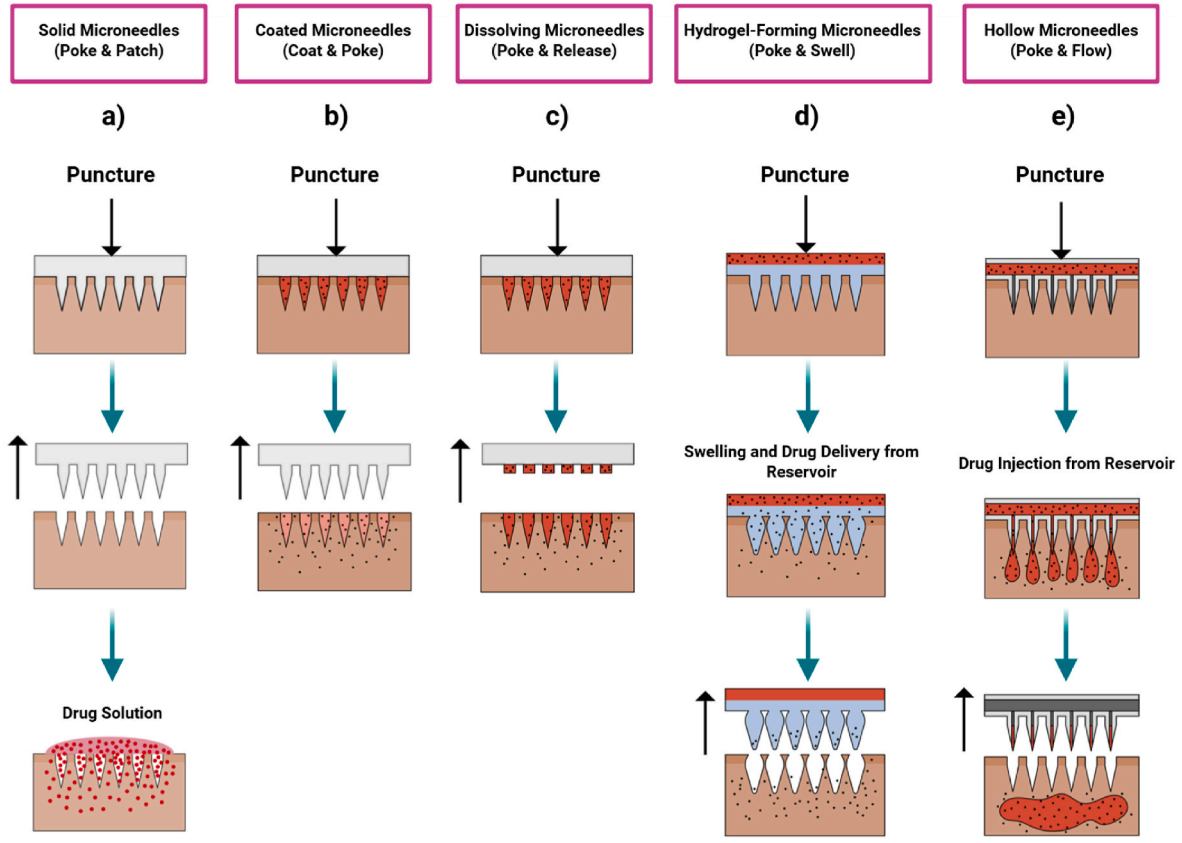

Fig. 2. A schematic representation of various types of microneedles. a) Solid microneedles. b) Coated microneedles. c) Dissolving microneedles. d) Hydrogel-forming microneedles. e) Hollow microneedles.

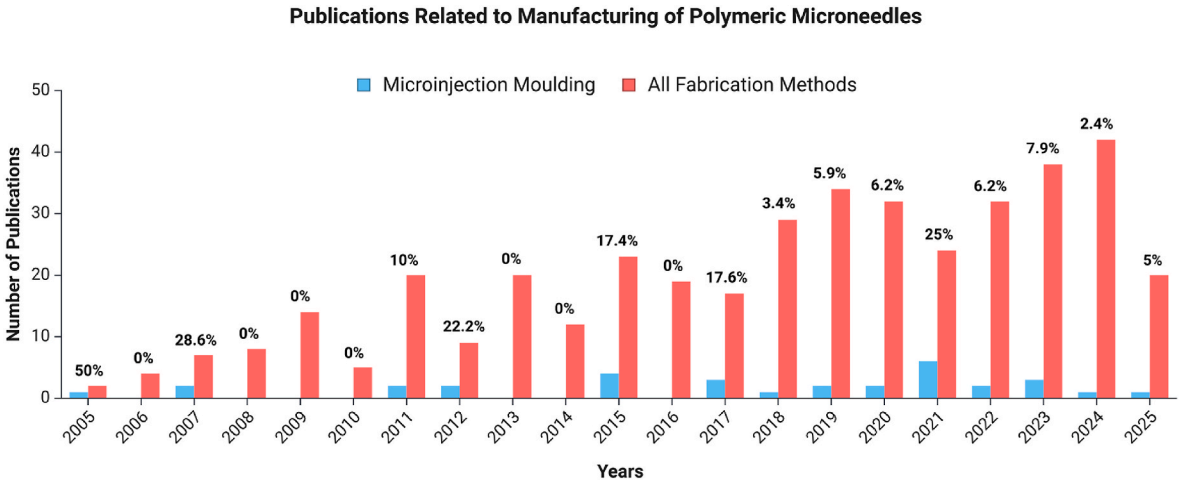

Fig. 3. Comparison of the number of research papers published from 2005 to 2025 on the fabrication of polymeric microneedles using microinjection moulding versus all fabrication methods. The percentage of publications using microinjection moulding relative to all fabrication techniques is indicated for each year. Data derived from Google Scholar and Clarivate Web of Science on August 7, 2025 [32].

acid (PLA), poly lactic-co-glycolic acid (PLGA), and Gelatin methacryloyl (GelMA), have been utilised to manufacture microneedles [34–40]. Polymers are less expensive and simpler to fabricate than other materials [41]. As most polymers are viscoelastic, the possibility of shear-induced breakage of microneedles inside the skin decreases compared to brittle materials like silicon [42]. Additionally, there is a great advantage that all types of microneedles, including solid, hollow, coated, dissolvable, and swellable, can be fabricated with polymeric materials [43].

Polymeric microneedles have shown adequate mechanical properties for skin penetration when designed and applied with optimum insertion parameters (e.g., velocity, force), and geometries (e.g., tip area) [44–47]. The low toxicity and biocompatibility of biodegradable polymers enable different drugs to be delivered into the body [48]. Thus, compared with other materials, polymers have numerous benefits, making them an ideal candidate for the fabrication of microneedles, particularly through microinjection moulding. Table 1 compares the advantages, disadvantages, and microneedle types for various

Table 1
A summary of advantages, disadvantages, and microneedle types for various microneedle materials [8,41,43,48–54].

Material	Advantages	Disadvantages	Microneedle types
Silicon	• Flexibility for fabricating in various shapes and sizes	• Complicated, expensive, and time-consuming manufacturing. • Brittle, potential to break during insertion.	Solid Hollow Coated
Metal	• Biocompatibility • Low cost • Robust mechanical properties	• Non-degradable • Post-processing requirement • High initial costs	Solid Hollow Coated
Ceramic	• Resistant to chemical corrosion and compression loads. • High hardness • Biocompatibility • Low friction	• Brittle, under tensile loads • Time-consuming manufacturing	Solid Hollow
Silica glass	• Suitable for research aims • Easy visualisation of fluid flow	• Brittle • Time-consuming fabrication	Hollow
Carbohydrate	• Biocompatibility • Biodegradability • Low toxicity • Low cost	• Requirement for thermal treatment in fabrication	Dissolvable
Polymer	• Adequate mechanical properties • Low cost • Biocompatibility • Low toxicity • Biodegradability • Chemical stability	• Lower mechanical strength than metal, silicon, and ceramic	Solid Hollow Coated Dissolvable Swellable

microneedle materials.

3. Geometry of microneedles

Geometrical dimensions such as height, tip diameter or width, tip angle, interspace between the needles and number of needles in an array play significant roles in the mechanical strength and insertion efficiency of the polymeric microneedles [55]. Studies showed that reducing the tip radius or tip angle increases insertion efficiency and decreases the force required to penetrate the SC [56,57].

Various microneedles with different geometrical features and shapes are illustrated in Fig. 4. Pyramidal microneedles with a low aspect ratio offer greater mechanical strength, which benefits mechanically weak materials. However, an overly low aspect ratio can make it difficult to form a sharp tip during fabrication, leading to reduced insertion efficiency (Fig. 4a) [58]. A low-density microneedle array is more effective than a dense one, as closely packed microneedles can lead to the 'bed-of-nails' effect, reducing individual penetration efficiency (Fig. 4b and c) [19,59]. Arrowhead polymeric microneedles can enhance the reliability of skin penetration by counteracting the skin's elasticity, enabling it to stay embedded at its deepest point of insertion (Fig. 4d) [60]. Tiered microneedle designs featuring needles of varying heights within a single array can help lower the insertion force by focusing the applied force on fewer microneedles at the specific duration of penetration (Fig. 4e) [61]. Turret polymeric microneedles, which feature sharp tips and broad bases, can effectively puncture the skin while offering enhanced mechanical strength (Fig. 4f) [61].

4. Manufacturing methods of polymeric microneedles

Microneedle fabrication techniques vary depending on their material composition and applications. Different methods have been used to manufacture polymer microneedles [62–64], such as microinjection moulding [65], hot embossing [66], casting [67], 3D printing [68], fused deposition modelling (FDM) [69], inkjet printing [70], two-photon polymerisation (TPP) [71], drawing lithography [72] and laser micromachining [16]. Janphuang et al. [65] developed

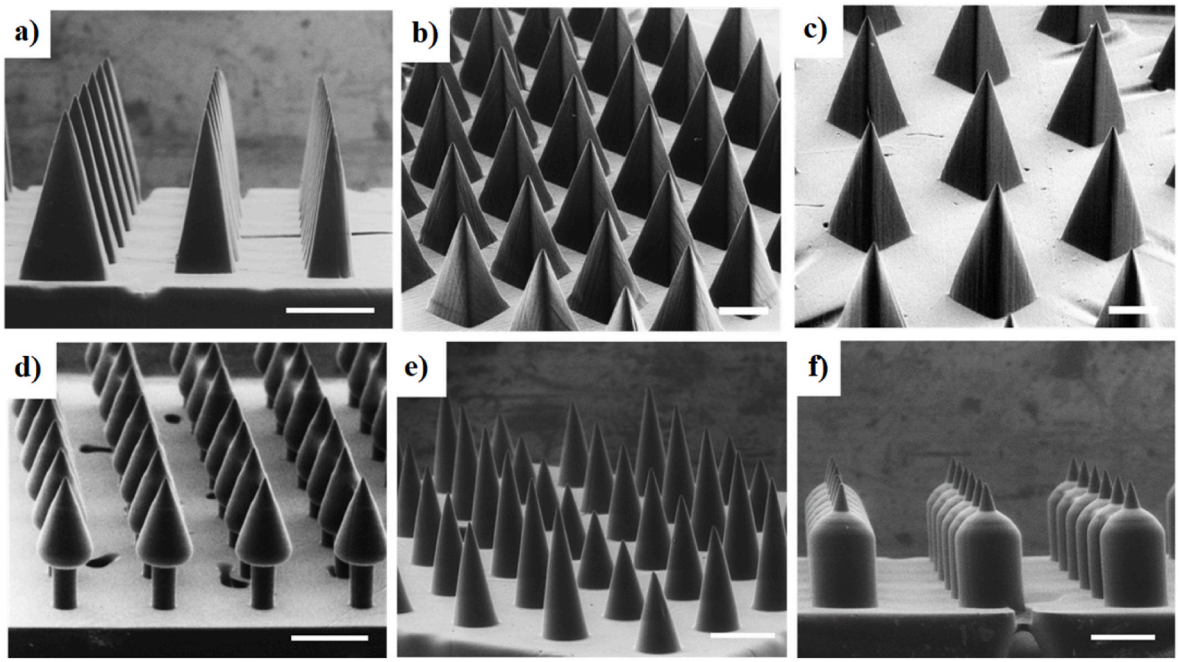

Fig. 4. Various geometries and shapes of microneedles. a) Microneedles with aspect ratios of 2, 3, and 4 (left to right). Microneedles with a height of 1000 μm and interspacing of b) 0.5 times base width and c) 1.5 times base width. d) Arrowhead microneedles. e) Tiered microneedles. f) Turret microneedles. Reproduced under the Creative Commons Attribution License (CC BY 4.0) [61], Copyright 2016, Plos One.

polymer-based microneedles using plastic injection moulding. The study investigated optimisation of injection moulding parameters such as clamping force, injection pressure and velocity to achieve the optimum reproducibility of solid microneedles from PMMA with round tip radius of 50 μm and height of 500 μm.

Both injection moulding and hot embossing manufacturing techniques have the potential for high production efficiency. In the hot embossing method, only the mould insert is required for replication; therefore, the initial expense is lower than that of injection moulding. However, due to the longer cycle time and subsequent operating steps, mass production by the hot embossing method could be more costly than injection moulding. On the other hand, in injection moulding, the initial tooling investment is more expensive than in hot embossing. Nevertheless, more significant product quantities with a lower price per product are obtained by injection moulding due to the quicker cycle time and fewer assembly steps of the micro-moulding machine than hot embossing.

Additive manufacturing methods like 3D printing provide affordable options for printing products in lower quantities. However, they have been unable to replace the injection moulding cost-effectiveness for mass production.

A comparison of cost per product versus the number of products for injection moulding, hot embossing, and additive methods is illustrated in Fig. 5. Overall, the hot embossing method is highly recommended for lower quantities with the aim of prototyping and testing, especially in academia. In contrast, the microinjection moulding method is more applicable to industrial environments and in solving supply chain issues related to medical devices [73]. Microinjection moulding offers great replication potential in micro-scale technologies, indicating that this method may be an economically optimal candidate for the mass production of microneedles [16,29,74].

5. Injection moulding fabrication process

Injection moulding has been considered a cost-effective manufacturing method that uses thermoplastic materials to produce products in large quantities [77]. In order to improve the performance of the fabrication procedure and the quality of products, several parameters should be considered and optimised. These parameters include pressure and speed of injection, mould temperature, injection and holding duration, and cooling procedure. Optimising the process parameters impacts the products' mechanical properties and geometrical features [78]. The injection moulding method has already been well recognised and utilised in various industrial sectors like automotive, aerospace, telecommunication, and biomedical due to its high accuracy, short cycle time, and low complexity of the production process [79].

5.1. Injection moulding steps

Injection moulding technique consists of four significant steps: a) plasticisation (melting), b) injection and clamping, c) moulding and cooling, and d) product ejection, as shown in Fig. 6. In the first step of the process, the plastic pellets are melted by a heating system to feed the material to the injection unit (Fig. 6a). Subsequently, as the required amount of molten material is provided, the thermoplastic material is pressurised and injected into the mould cavity which is securely closed by the clamping unit (Fig. 6b). In the next step, the material filling the mould area is cooled down to finalise the solidification of the desired 3D shape (Fig. 6c). Finally, the product is ejected and demoulded by opening the clamping unit (Fig. 6d) [78]. The machine continuously repeats the cycle to create more products. In mass production, a shorter cycle time will lead to lower costs and higher product output [80]. With the feasibility of automation, low operational costs, and the flexibility of 3D mould geometry, this fabrication process is well-suited for large-scale production [81].

5.2. Mechanism of a typical injection moulding machine

Typically, an injection moulding machine consists of an injection unit, a clamping unit, and a mould of the desired product geometry (Fig. 7). The injection unit includes a pellet reservoir, a reciprocating screw, and an injection nozzle. As the plastic pellets enter the heated barrel, they are homogenously melted. Subsequently, the molten material is injected under high pressure through the nozzle into the mould cavity using a rotating screw, which runs with an electrical or hydraulic

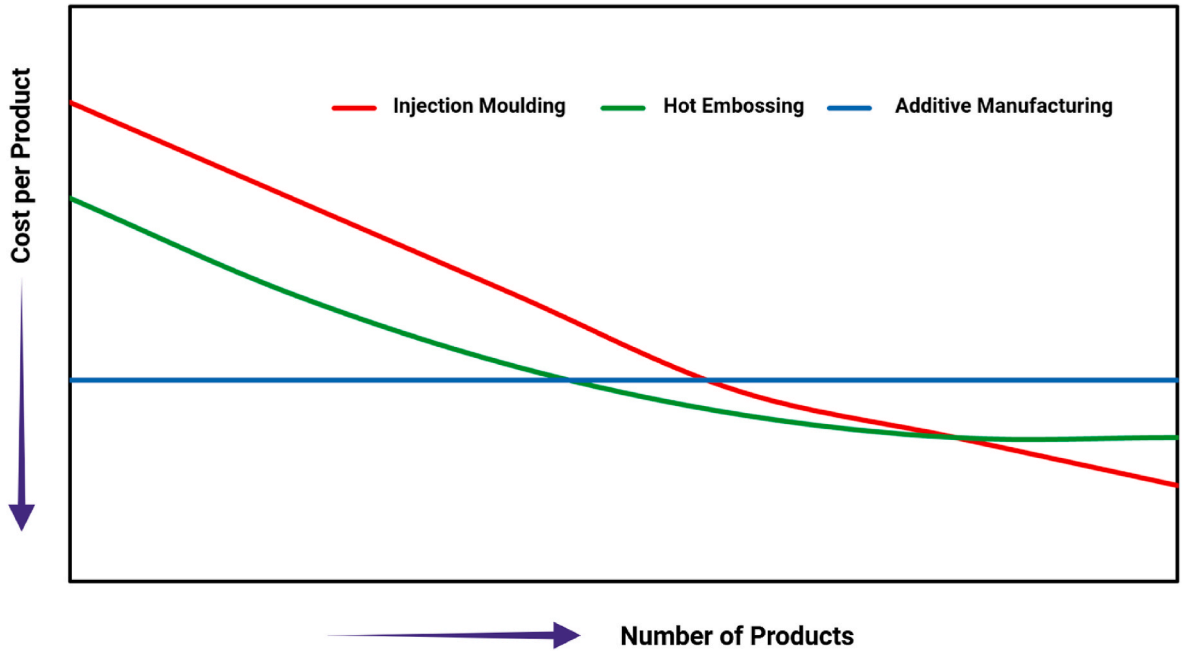

Fig. 5. Comparison of cost per product versus the number of products produced from injection moulding, hot embossing and additive fabrication methods, redrawn based on [73,75,76].

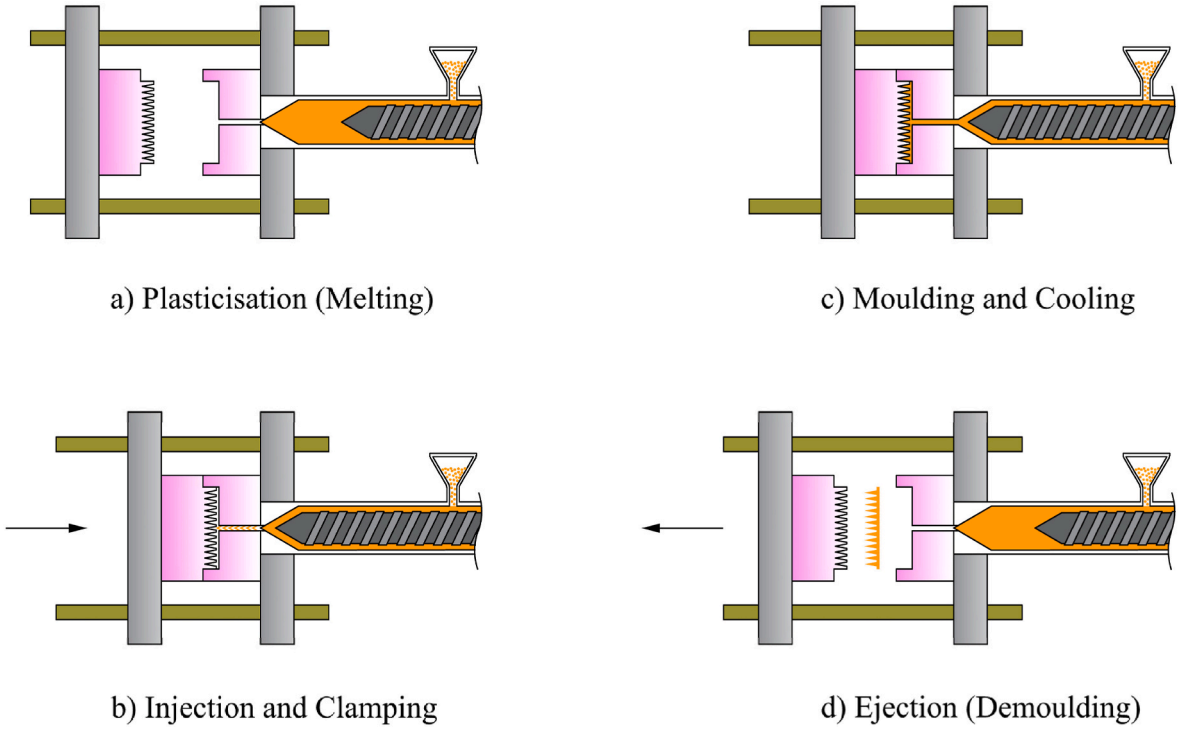

Fig. 6. The schematic of the injection moulding process. a) Melting of thermoplastic pellets into the injection unit. b) Injection of pressurised molten material into the mould cavity while applying clamping force. c) Moulding and cooling the molten material for solidification. d) Demoulding the final product.

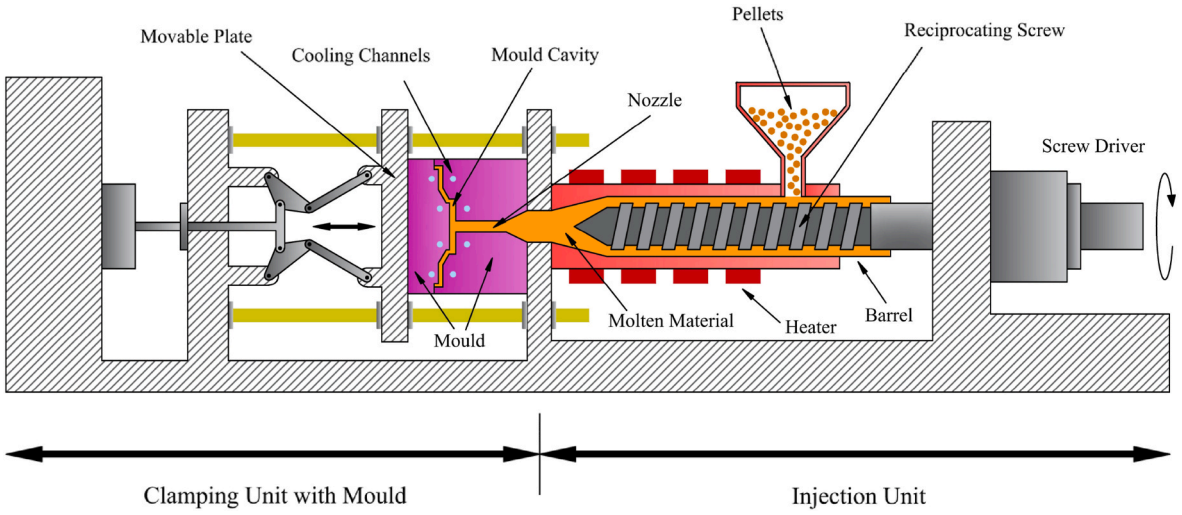

Fig. 7. The schematic of a typical injection moulding machine, including the injection unit, clamping unit, and mould.

driver. The two halves of the moulds are connected to movable and stationary plates and contain the cavity with the shape of the desired product geometry [82]. There are also cooling channels around the mould cavity containing the stream of coolant, which cools down the liquid thermoplastic material to form the solid shape of the ultimate manufactured product [83]. On the other side of the machine, the clamping unit's primary duty is to apply force and press the mould halves tightly while injecting pressurised molten material. Furthermore, at the final stage, the clamping unit is opened to eject the final product when the moulded material is completely cooled and solidified [84]. Accordingly, the clamping unit's performance significantly influences product quality. The toggle type is the most common clamping mechanism in injection moulding devices [85].

6. Insights from microinjection moulding of polymeric microdevices for microneedle fabrication

The fundamental principles of microinjection moulding, including process parameters, optimisation approaches, and machine considerations, are similar across a wide range of thin-walled polymeric microdevices, such as microneedles, micro-rings, microfluidic chips, micropatterns, and micro-pillars. Despite differences in mould geometries, the underlying manufacturing process is similar, and insights gained from these applications can be directly applied to microneedle production. This broader perspective provides a more comprehensive understanding of the capabilities and limitations of injection moulding at the micro-scale.

Downsizing of products to combine all technical features in micro/

nano sizes is a remarkable improvement in modern technologies. Due to the enormous demand for microelectromechanical systems (MEMS) and microsystems (MST) in the market, there is a fundamental need to find a reliable replication technique to mass-produce micron-sized components. The fabrication technique of microinjection moulding has been successfully applied to manufacture micro-scale polymeric systems with complicated geometries for different applications like drug delivery, medical implants, microlens arrays, microfluidic devices, microstructured surfaces, and micro-optics, all with the aim of mass production [86,87].

Micro-moulding refers to fabricating parts with milligrams and micrometres' weight and dimension ranges [88]. Various types of thermoplastic polymers or nanocomposites, such as PMMA, cyclic olefin copolymers (COC), polystyrene (PS), PP, and PC, PLA, Polyethylene (PE), and linear low-density polyethylene (LLDPE) have been widely used for the fabrication of microdevices using microinjection moulding due to the low cost, manufacturing flexibility, and excellent replication capabilities [89–93]. Polymers with low viscosities and high flow rates are suitable for microinjection moulding. One of the challenges related to producing micro-scale products using the injection moulding method is the requirement for a highly accurate machine to adjust and optimise the injection parameters precisely [94].

6.1. Technology development of microinjection moulding machines

The development of the microinjection moulding process commenced in the last few decades by modifying industrial hydraulically driven machines. Further evolution in micro-machines was accomplished in the middle of the 90s to ensure process consistency of micropart fabrication [95]. The downscaled, single-stage injection moulding system follows the same technology as the large-scale injection moulding machines. The two tasks of reciprocating screws in micro-machines are to plasticise pellets and inject the melt into the mould as well as the macro-machine. In micro-scale machines, in order to improve the accuracy of melt injected and prevent polymer degradation, the dimensions of the injection unit components, including screw and barrel diameters, are diminished. Nevertheless, the least effective diameter of the screw should be 14 mm to prevent shear failure. In addition, the channel depth of the screw should be proportional to the standard size of thermoplastic grains and the plasticisation requirements. Measuring the amount of molten material required for injection is challenging in a single-stage micro-machine. For instance, in order to provide a shot size of 1 mg, only the movement of 0.0056 mm of a reciprocating screw with a diameter of 14 mm is required, which is a challenging degree of adjustability [87,88,96].

In double-step microinjection moulding machines, the conventional reciprocating screw is replaced with the combination of a screw for polymer plasticisation and a separate small plunger for metered melt injection to overcome the obstacles of single-step machines. It alternatively works with a two-stage plunger consisting of a plasticiser and shooting plungers. Therefore, in two-step micro-machines, by utilising an injection piston with a few millimetres diameter, the small amount of injected melt is more controllable and accurate and higher injection velocity will be achieved in similar displacements [96]. Moreover, other types of micro-machines defined as "three-step" systems, separated components consisting of a plasticisation screw, an injection plunger, and a metering piston, are embedded in order to improve the metering accuracy and to minimise the melt cushion and cold material slug [87].

6.2. The potential of using conventional injection moulding machines for micro-fabrication

Some polymeric microdevices can be fabricated by either microinjection or conventional injection moulding machines [97]. However, micro-machines have higher efficiency and can resolve the major drawbacks related to the manufacturing of microparts utilising large-scale injection moulding machines. There is a limitation for dimensional tolerances of microparts (up to a few micrometres) with conventional injection moulding machines, so it is difficult to achieve precise process replication and the required properties [98]. In addition, the process of micropart demoulding is sensitive and may not be practical using the ejection system of macro-machines. Furthermore, the diameter of injection screws of conventional machines is not small enough to inject the required small shot size of polymer with greater speeds per cycle which reduces the metering accuracy and increases the waste of material. Accordingly, the total expenses of the procedure will rise, particularly in the case of using costly materials for medical applications. Meanwhile, the duration of the fabrication cycle will also increase, and polymer degradation may occur due to the remaining material in the barrel. On the other hand, it is possible to observe the backflow of molten material, especially at higher pressures [88,99].

Baruffi et al. [100] analysed the replication precision using microinjection moulding and conventional moulding machines with a thermoplastic elastomer. The study used two different moulds with similar micro-cavities: a normal-sized mould equipped with microcavities for conventional machines and a micro-sized mould for the micro-machine. The results demonstrated a reduction in wasted material in the micro-machine. In addition, the more accurate amount of injected polymer, mass balance, and homogeneous density in various parts of the mould cavity was observed. Furthermore, results showed that greater replication accuracy is achieved by a microinjection moulding machine [97]. Nevertheless, conventional injection moulding machines can be used in the laboratory fabrication of low-quantity microparts, notwithstanding time and cost factors.

7. Microinjection moulding strategies for fabrication of polymeric microneedles

Microinjection moulding for the fabrication of microneedles as a drug delivery tool has been studied to address mass-scale production challenges. Various studies have investigated mould manufacturing and thermoplastic micro-moulding to achieve a reasonable replication fidelity of microneedle arrays. The process chain for microneedle manufacturing, including design, mould fabrication, microinjection moulding, and quality assessment, is illustrated in Fig. 8.

Different thermoplastic materials such as acrylonitrile butadiene styrene (ABS) [16], PP [101], COC [21], cyclic olefin polymer (COP) such as Zeonor 1020R [24], PC [102], polyethylene terephthalate (PET) [103], PMMA [104], polyglycolic acid (PGA) [105], PLA [106], PLGA [31], and polyether ether ketone (PEEK) [29] have been used for the fabrication of microneedles using injection moulding. However, some pure materials like PLA require modification to improve microneedles' mechanical strength. For example, Zhang et al. [107] fabricated microneedles using a mixture of 90 % PLA and 10 % poly(p-dioxanone) (PPDO) to enhance the mechanical properties of microneedles. Table 2 contains the properties of several thermoplastics used for the fabrication of microneedles.

7.1. Technology development of microneedle microinjection moulding

Solid and hollow microneedles are the most common types fabricated using microinjection moulding. Nevertheless, other novel-shaped microneedles, such as semi-hollow and bird-bill arrays, have also been manufactured through this methodology [25]. Techniques like piezoelectric inkjet coating and dip-coating have been employed to deposit drugs on mould-injected solid microneedles [24,27,105]. The microinjection moulding technologies used to fabricate microneedles can be divided into two main categories: conventional and ultrasonic, based on the plasticisation mechanism, as shown in Fig. 9.

7.1.1. Conventional microinjection moulding of microneedles

In conventional micro-moulding, the polymeric material is

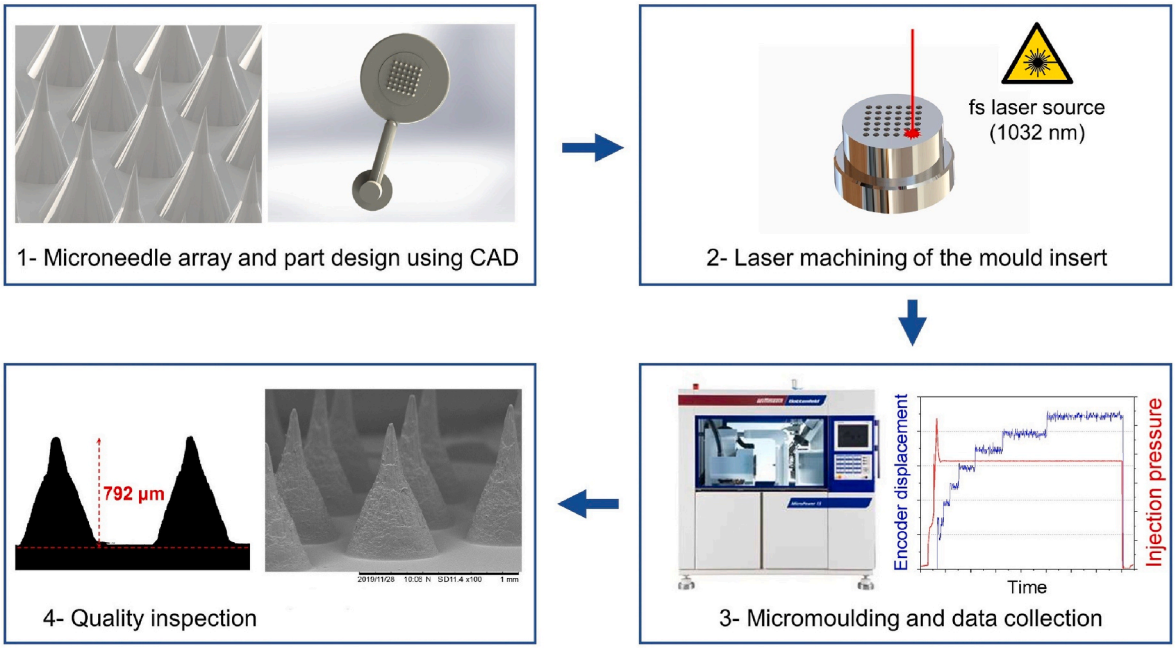

Fig. 8. Manufacturing process chain of polymeric microneedles through injection moulding method, 1) microneedle array and part design, 2) laser micromachining of negative metal mould, 3) fabrication of microneedles using microinjection moulding machine, 4) quality assessment of micro-injected microneedles. Adapted with permission from Ref. [16], Copyright 2021, Elsevier.

Table 2
Thermoplastic materials and their properties for the fabrication of microneedles via the microinjection moulding method.

Thermoplastic material	Melt Flow Rate (MFR)	Density (g/cm^3)	Other properties	Ref.
Acrylonitrile Butadiene Styrene (ABS) resin grade HMG94MD	11.7 g/10 min @ 220 °C/ 5.0 kg	1.06	• Tensile strength at yield: 46 MPa • Shrinkage: 0.5–0.8 % • Glass transition temperature: 106.7 °C	[16]
Polypropylene (PP, GA12)	12 g/10 min @ 230 °C/ 2.16 kg	0.895–0.92	• Tensile strength at yield: 34 MPa • Shrinkage: 1–2.5 % • Heat deflection temperature at 0.45 MPa: 90 °C	[101, 108]
Polypropylene (PP, 578 N)	24.5 g/10 min @ 230 °C/ 2.16 kg	0.928	• Tensile strength at yield: 42 MPa • Tensile modulus: 2100 MPa • No-flow Temperature: 109 °C	[102]
Polycarbonate (PC, HPX8REU)	35 g/10 min @ 300 °C/ 1.2 kg	1.188	• Tensile strength at yield: 59 MPa • Tensile modulus: 2360 MPa • No-flow Temperature: 147 °C • Glass transition temperature: 141 °C	[102, 109]
Polymethyl methacrylate (PMMA, Plexiglas 8N)	3 cm^3/10 min	1.19	• Tensile modulus: 3300 MPa • Glass transition temperature: 117 °C	[17]

plasticised by a plasticisation screw, as described in section 7.1. Several studies were conducted on standard machines to achieve a reliable pathway for high-quality microneedle replication. For example, Sammoura et al. [110] designed and fabricated in-plane and open-channel polymeric microneedles to optimise the process's temperature, injection speed and pressure, and clamping force. The researchers used Moldflow software to analyse the relation between filling duration and ultimate injection pressure. A comparison showed a discrepancy in the filling time parameter between experimental and numerical data. The main reason was the inability to control the mould temperature during the actual test. Also, the roughness of the mould surface was not included in the model. The results highlight that developing a simulation algorithm and tracking the mould temperature during the experiment can improve the numerical results [110].

Gülçür et al. [16] investigated the replication of 6 × 6 solid microneedle arrays with commercial ABS resin as a biocompatible material using a Wittmann-Battenfeld Micropower 15 micro-moulding machine. The machine consists of a 14 mm plasticisation screw which is suitable for standard pellet sizes and a 5 mm injection piston that makes the dose of injected melt more precise. The fabrication was performed at two different packing pressures of 750 and 1100 bar, with identical mould and melt temperatures, injection speeds, and packing durations. The ideal height of products without any flashing impact was observed to be obtained at the maximum possible pressure, as illustrated in Fig. 10a. The results showed that by increasing the pressure, the efficiency of microneedles' replication improves, and there is a reduction in the quality of microneedles' dispersion. A smaller tip radius was also acquired at higher pressure, as shown in Fig. 10b. Furthermore, the extracted information, such as injection pressure, piston location, and mould cavity pressure during production, was used to analyse the process parameters that impact the final product. Various sensor technologies, including high-speed thermal cameras, cavity pressure transducers, and controllers, were used to monitor the in-line processing data. Baruffi et al. [111] also used the same strategy for monitoring the microinjection moulding procedure to study the relation between the injection pressure and dimensional accuracy of the micropart.

In another study, Evens et al. [20] produced cone-shaped microneedles from PP grade 515A using a hydraulic injection moulding

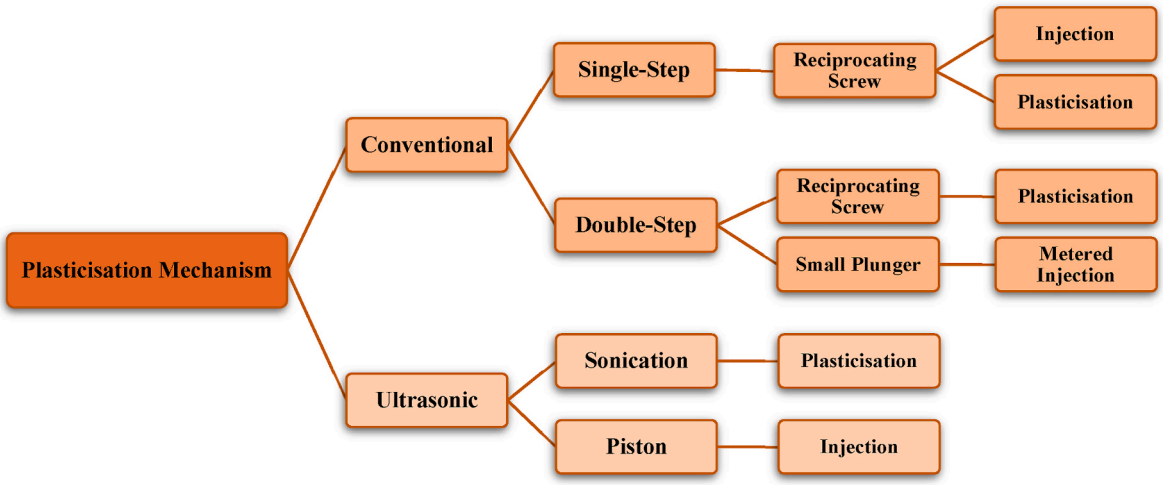

Fig. 9. Classification of microinjection moulding machines used to fabricate polymeric microneedles [87,108,110].

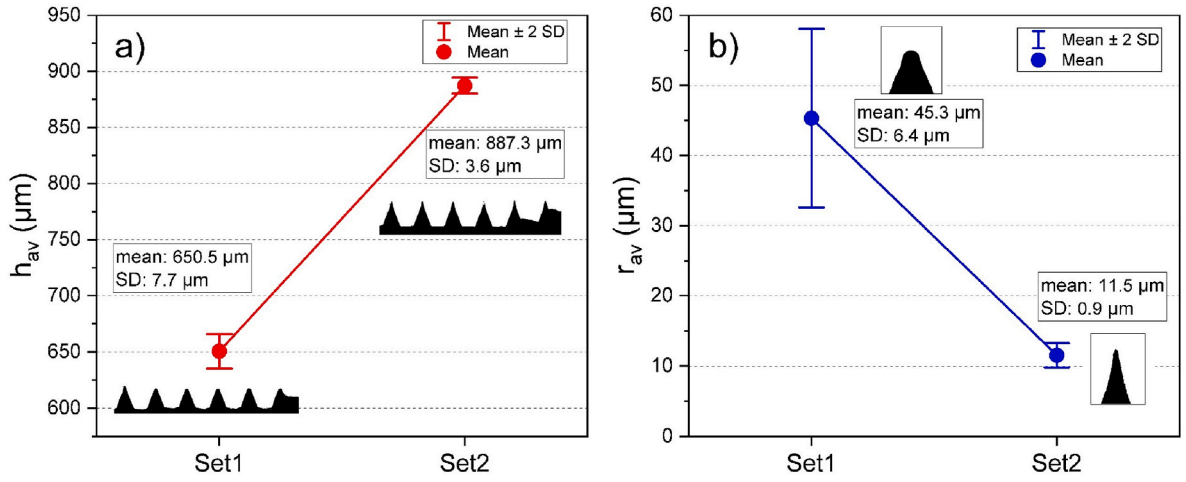

Fig. 10. Comparison of average geometrical features measured for each 6 × 6 microneedle array considering packing pressures of 750 bar (set 1) and 1100 bar (set 2). a) The average microneedle's height. b) The average tip radius. Reproduced with permission from Ref. [16], Copyright 2021, Elsevier.

machine, creating solid microneedles with tip radius smaller than 20 µm for drug delivery applications. In another study by Evens et al. [102], the PP and PC microneedles were replicated using the same machine, showing that the PP microneedles' replication fidelity was greater than the PC. It also showed a linear relationship between the microneedles' height and depth of cavities.; the higher the aspect ratio, the lower the replication of the microneedles. The main reasons are the hesitation effect and early melt solidification due to the increment of heat transfer in narrower parts of the cavity. The hesitation effect occurs when the polymeric material stagnates at narrow sections and does not incline to fill the slender parts of the mould completely, which may also intensify rapid freezing [112,113]. Strategies like air vacuuming from the cavity during the filling step and using supercritical carbon dioxide fluid to reduce the melt viscosity can improve the filling efficiency [114].

Creating microneedles with sharp tips and high aspect ratios is still challenging in microinjection moulding. A more homogeneous melt distribution inside the mould cavities can be achieved by introducing a compression stage. Hence, replacing the injection compression moulding method can overcome the problems related to conventional microinjection moulding [115]. In this technique, when the melt is injected into the cavity, the two halves of the mould are not entirely closed. Then, after filling 90 %–98 % of the thermoplastic material, the mould is fully closed and compresses the cavity melts, leading to homogeneous distribution. However, using this strategy is more complicated than conventional injection moulding and the parameter of "compression stroke" as the extra gap between the moulds should be optimised. Evens et al. [109] equipped the conventional microinjection machine with an injection compression module to utilise the same machine for both methods. They concluded that the replication fidelity of the same type of microneedle arrays by compression and conventional strategies is 79 % and 70 %, respectively, as shown in Fig. 11.

Manufacturing hollow polymeric microneedles using standard moulding techniques is also challenging. Some post-processing methods, such as laser ablating and X-ray exposure, may be used to create fluidic channels inside the microneedles [22,104,116–118]. In order to eliminate complicated post-fabrication procedures, Lippmann et al. [21] developed a technique for producing in-plane hollow microneedles, a combination of conventional injection moulding and investment casting. In this three-stage approach, the investment components were first aligned with the mould insert to define the hollow channels of microneedles. Secondly, the thermoplastic material was mould-injected into the micro-structures around the investment. In the last step, the fabricated part is demoulded, and the interior investment part is dissolved to finalise the fabrication of hollow microneedles. In other studies, the hollow microneedle cavities were laser ablated precisely on moulds to replicate polymeric hollow microneedles directly through conventional

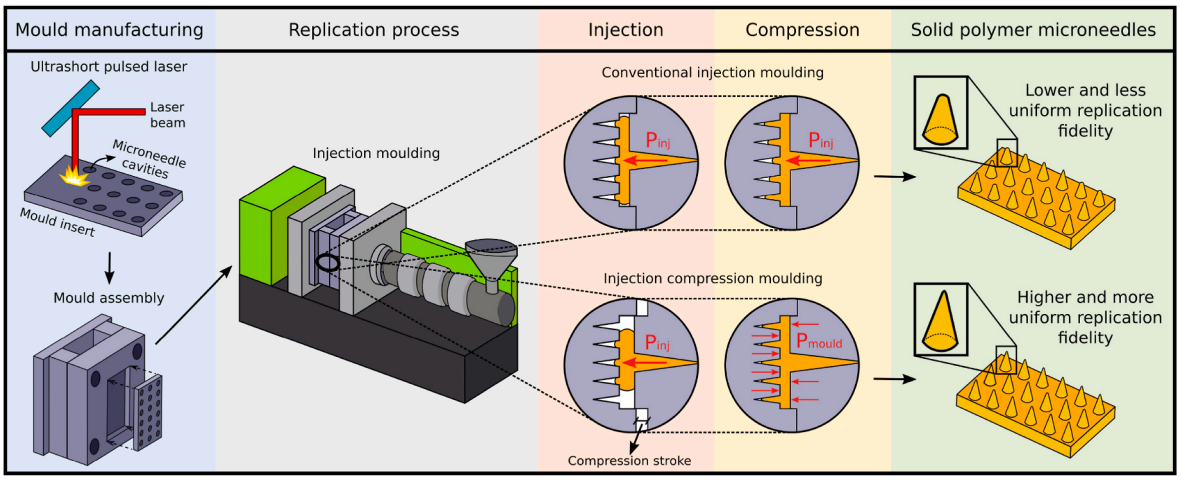

Fig. 11. Comparison of replication fidelity of solid microneedles fabricated by compression and conventional injection moulding. Reproduced under the Creative Commons Attribution License (CC BY 4.0) [109], Copyright 2022, MDPI.

injection moulding methods without any post-processing or investment techniques. In some studies, micro-hole drilling on polymeric base plates was still required to connect the needles' internal bore to a flat surface. It was concluded that the replication fidelity improves with simultaneous higher mould temperature, volumetric injection rate, holding pressure, and melt temperature [17,119].

Several heating methods, including flame heating [120], electric heating [121], steam heating [122], and infrared heating [123], were considered to increase the mould temperature in the microinjection moulding rapidly. As a form of radiation, the infrared heating technique attracts more attention due to its safety and energy-saving. Furthermore, it is not required to modify the mould system significantly in the case of infrared heating. Gao et al. [124] developed an infrared heating system using various reflector types to improve the heating efficiency of the microneedle mould. The results indicated that the surface temperature of the mould insert increased from 19.96 °C to 174.14 °C in 25 s, while there was not much temperature gradient in different parts of the cavity. The fabrication assessment demonstrated that the average height of uniform mould-injected microneedles rose by 35.78 %. Moreover, the shrinkage of microneedles was also decreased using the infrared heating system.

7.1.2. Ultrasonic microinjection moulding of microneedles

Ultrasonic microinjection moulding technology is a recent development in the field in which plasticised materials are processed using ultrasonic energy instead of a conventional mechanical screw. Compared with standard systems, ultrasonic micro-moulding machines are more efficient in terms of energy consumption and material saving. Moreover, by this mechanism, an extremely short residence time is achievable as the thermoplastic material is exposed to high-value temperatures for a short duration, avoiding polymer degradation. Compared to the conventional method, higher cavity temperatures and pressures are observed after the filling step, demonstrating that the technology can be a viable alternative due to its superior replication fidelity [108,125].

Gülçür et al. [101] studied the effect of three different design factors, including sonication time, injection force, and mould temperature, on the replication efficiency of 5 × 5 polypropylene microneedles replication using an ultrasonic microinjection moulding machine which was equipped with an ultrasonic power generator. The injection axis was placed vertically in this mechanism. The polymer feedstock was located among the 8 mm injection piston and a sonotrode, generating ultrasonic vibrations while applying the pressure needed to push the material into the mould cavities through the feeding channels. Therefore, as the plunger moved up, the material was compressed, plasticised by sonication, and injected into the mould cavities. The measurement of microneedle height was performed using a telecentric optical imaging technique. It was concluded that increasing the mould temperature is the most influential parameter to improve the filling efficiency; however, regarding the heat deflection problem of PP material in the ejection step, the maximum possible amount of this variable is 90 °C. The mould insert was designed within the circular mould, which contains a 5 × 5 array of cone-shaped microneedle cavities with a depth of 550 μm, as illustrated in Fig. 12a. The average depth of the fabricated microneedle cavities was 535 μm. Fig. 12b displays the telecentric image of the PP microneedles fabricated using the ultrasonic microinjection moulding method, illustrating an example of height measurement [101].

In another study, an ultrasonic vibration system was tested by Gao et al. [126] to improve the quality of mould-injected microneedle arrays. This mechanism included a controllable ultrasonic generator, ultrasonic horns, and transducers placed on the movable part of the mould. Sustainable ultrasonic vibration was applied to the mould during injection, packing, and cooling. The results showed that the melt filling time was reduced by 31.25 % without notable changes in filling order over the cavity regions. Furthermore, the ultrasonic vibration could reduce the melt viscosity, particularly in regions away from the edges. Regarding mechanical properties, it was found that, in optimum excitation voltage, the hardness and Young's modulus of PP microneedles rose by 20.4 % and 7.7 %, respectively.

A detailed summary of reported microinjection moulding data for fabricating polymeric microneedles, including machine model, thermoplastic material, mould material and fabrication technique, melt and mould temperature, injection parameters, packing pressure, and outcomes, are presented in Table 3.

7.2. Development of microneedles negative mould for microinjection moulding

Mould manufacturing for microneedles is a critical step in achieving precise geometry and high replication accuracy in the microinjection moulding process. Identifying a fabrication method to produce the negative metal mould for microneedles with precision, low cost, and reasonable time is complicated. The accuracy of the mould manufacturing technique plays a prominent role in achieving smooth surface finishing and precise geometry of cavities, which further affect the microneedle dimensions, particularly its aspect ratio and tip area. Micromachining techniques such as laser ablation [129], micro-electrical discharge machining (μ-EDM) [65,128], milling [130], numerical control (NC) machining [110], and drilling [124] have been used to fabricate negative metal moulds. In addition, lithography,

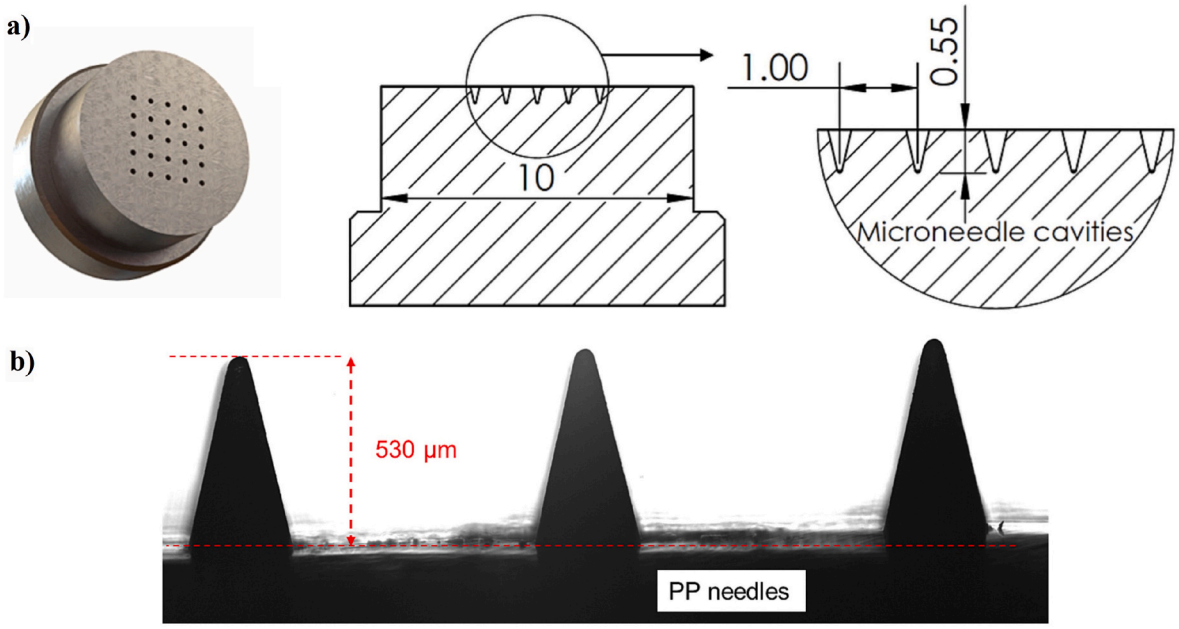

Fig. 12. The mould insert design and image of microinjected microneedles. a) A 5 × 5 configuration design of cone-shaped microneedle cavities and a cross-sectional view of the geometrical features. b) The telecentric image of polypropylene (PP– GA12) microneedles fabricated using an ultrasonic microinjection moulding method. Adapted under the Creative Commons Attribution License (CC BY 4.0) [101], Copyright 2023, Elsevier.

electroplating, and moulding (LIGA) utilising deep X-ray exposure have also been investigated for fabricating micro-cavities with high aspect ratios [65]. The mould inserts can be manufactured via poly 2-Hydroxyethylmethacrylate (pHEMA)/epoxy transfer casting or resin 3D printing. Compared with metal mould inserts, these methods and materials reduce the complexity and expenses of prototyping, allowing easy modification of the mould inserts' geometry. However, due to their low durability, these materials are well-suited for research studies [131]. Also, as Polydimethylsiloxane (PDMS) moulds can be deformed easily, they are not suitable for common injection moulding. However, by modification of the technique and applying a vacuum system instead of high pressure, PDMS moulds can be applied. In this case, air is removed from the mould, and the melted polymer fills the cavities [26].

7.2.1. *Laser micromachining*

According to the literature, the laser ablation technique is mostly used to produce metal mould cavities of microneedles. An optical laser beam removes materials from a substrate to fabricate the desired shape in the laser machining process. As the process is non-contact, the wear effect of the tool does not appear, and the product has low heat deposition [132,133].

7.2.1.1. Mould fabrication for solid microneedles replication. Gülçür et al. [16] utilised a laser micromachining method to fabricate the conical-shaped mould for a microneedle array at 1 mm pitch with a depth and base diameter of 900 µm and 630 µm, respectively. The mould cavity plate was manufactured from P20 tool steel equipped with heaters and thermocouples to control the mould temperature. Stavax® ESR steel was used as the mould material which is suitable for microinjection moulding due to its good polishing, machining, and wear resistance properties. The layer-by-layer laser micromachining mechanism was employed to make mould cavities using a femtosecond laser, which was merged into a multi-axis machining system. The average depth of needle cavities and tip radius were 912 µm and 5.2 µm, respectively. The duration of micromachining of 36 microneedle cavities was 40 min, which was significantly lower than other techniques.

In another work with a low-corrosion tool steel (grade 1.2083–AISI 420) mould material, the laser machining of 3 × 3 micro-holes was conducted in layers of 150, 300, 450, and 600. It was specified that increasing the number of layers increases the hole depth and base diameter. The replication of microneedles using microinjection moulding showed that the microcavities were not entirely filled by polymers, which caused a larger tip diameter. The results showed that as the number of layers in the laser ablating of mould metal increases, a lower volume of polymeric material fills the cavity, which leads to a larger tip radius. For instance, in cases of 150 and 600 layers, the average tip radius of microneedles was 10.3 µm and 19.6 µm, respectively [20]. Besides variation of laser ablation layers, cavities with various base diameters were also laser machined using a cross-hatching strategy by Evens et al. [102] on three different metal moulds, including tool steel, copper alloy, and aluminium alloy, to investigate the impacts of mould variables on the geometry of the microneedles mould. The base diameter of designed 3 × 3 micro-cavities varied from 100 µm to 400 µm with steps of 100 µm. The cross-sectional images of microneedles using a micro-computed tomography (µ-CT) system are shown in Fig. 13a. The mould inserts were ultrasonicated in an ethanol bath to remove residual material after laser machining. In order to form cavities with extremely low tip areas and prevent plasma shielding effect and laser reflectance, the cone-shaped geometry was designed for micro-cavities. As identical strategies were considered for machining all studied materials, it was observed that material properties like heat capacity, thermal conductivity, electron-phonon coupling constant, and absorptivity influenced the geometry of cavities. For instance, the aspect ratio of an aluminium alloy mould was noticeably smaller than that of tool steel and copper alloy due to the lower electron-phonon coupling constant and thermal conductivity of aluminium, which led to poor replication fidelity in microinjection moulding. Although it is easier to form aluminium on a micro-scale, this material is not frequently used for injection moulding. Femtosecond laser ablation of metal moulds is more appropriate for metal materials with high electron-phonon coupling constant and high thermal conductivity. A comparison of the hole diameter on the surface of each mould material with the machining layer is shown in Fig. 13b. The higher the number of layers, the larger the hole diameter. The analysis of the maximum relative standard deviation between the designed and obtained hole diameters showed acceptable repeatability of the process; however, these deviations are not desired in some

Table 3
A summary of reported input parameters and outcomes of experimental microinjection moulding polymeric microneedles using commercial machines.

Machine Model	Polymer	Mould Material	Mould Fabrication Technique	Melt Temp. (°C)	Mould Temp. (°C)	Injection Parameters	Packing/ Holding Pressure	Fabrication Outcomes, Comparison, or Purpose	Ref.
Wittmann-Battenfeld Micropower 15	Acrylonitrile Butadiene Styrene (ABS) resin grade HMG94MD	Stainless steel (Stavax ESR)	Laser micro-machining	235	60	Injection velocity: 400 mm/s	1100 bar	Average microneedle height and tip radius: 887.3 and 11.5 μm	[16]
Sonorus 1G (Ultrasonic) Sonication amplitude: 96 μm	polypropylene (PP–GA12)	Stainless steel (Stavax ESR)	Electrical discharge machining (EDM)	N/A	90	Injection force: 900 N	N/A	Average microneedle height: 530 μm	[101]
Engel ES 200/ 35 HL	Polypropylene (PP, 578 N)	Tool steel 1.2083, Copper	Laser micro-machining	240	80	Volumetric injection rate: 149 cm^3/s	575 bar	Replication fidelity of PP was higher than PC, considering all three mould materials	[102]
	Polycarbonate (PC, HPX8REU)	AMPCOLY 940, Aluminium 3.4365		315	115		749 bar		
Engel ES 200/ 35 HL	Polymethyl methacrylate (PMMA, Plexiglas 8N)	Aluminium zinc alloy (grade 3.4365)	Laser micro-machining	260	110	Volumetric injection rate: 150 cm^3/s	800 bar	Efficiency of filling inside the cavity: 79 %	[17]
Engel ES 200/ 35 HL	polypropylene (PP grade 515A)	Tool steel (grade 1.2083)	Laser ablating	240	80	Volumetric injection rate: 128 cm^3/s	475 bar	Microneedle height and tip radius: 1307 and 19.6 μm, considering 600 layers of laser ablating Microneedle height and tip radius: 912 and 10.3 μm, considering 150 layers of laser ablating	[20]
Sonorus 1G (Ultrasonic) Sonication amplitude: 96 μm	polypropylene (PP–GA12)	Stainless steel (Stavax ESR)	Laser machining	290	90	Injection force: 750 N, injection pressure: 149.3 bar	N/A	Average microneedle height: 856 μm	[108]
FANUC Roboshot α series 30iA	Topas (COC)	Aluminium	NC machining	230	55	Injection pressure: 17000 Psi	First step: 2000 Psi, second step: 3000 Psi	Discrepancy between experimental and numerical results due to the inability to control the mould insert temperature during experiments	[110]
Battenfeld Micro-Power 5	Polylactic acid (PLA)/ Poly p-dioxanone (PPDO) (90/10)	N/A	N/A	180	40	Injection velocity: 100 mm/s, injection pressure: 1500 bar	N/A	Fabrication of PLA-based blend microneedles to improve mechanical properties compared to pure PLA	[107]
Sesame moulding machine	Polyglycolic acid (PGA)	Steel	N/A	238	Fixed mould: 41 Moving mould: 29	Injection velocity: 160 mm/s, injection pressure: 13.79 MPa	First step: 5.17 MPa, second step: 2.69 MPa	Prepare microneedles for inkjet-deposited antifungal coatings	[105]
SP-5	Polyoxymethylene (POM)	SS 420 heat-treated stainless steel	Laser machining	180	110	Maximum injection velocity: 120 mm/s	First step: 900 bar, second step: 150 bar	Hollow microneedle height: 500 μm	[127]
MircroPower-5t	PMMA	High-temperature alloy steel (SKD11)	Electrical discharge machining (EDM)	230	50	Volumetric injection rate: 9 cm^3/s, injection pressure: 120 MPa	60 MPa	Microneedle height and tip radius: 500 and 50 μm	[65]
FANUC ROBOSHOT S-2000i 50B	PP	N/A	N/A	230	50	Injection velocity: 30 mm/s	30 MPa	Improvement of mould filling efficiency and enhancement of mechanical properties using ultrasonic vibration on mould	[126]
	PMMA			250	60		50 MPa		
Battenfeld Micro-Power 15	Polyether ether ketone (PEEK, LT-3)	Stainless steel (Stavax ESR)	Electrical discharge machining (EDM)	400	210	Maximum injection velocity: 750 mm/s	600 bar	Microneedle shaft length and tip radius: 556 and 32 μm	[128]

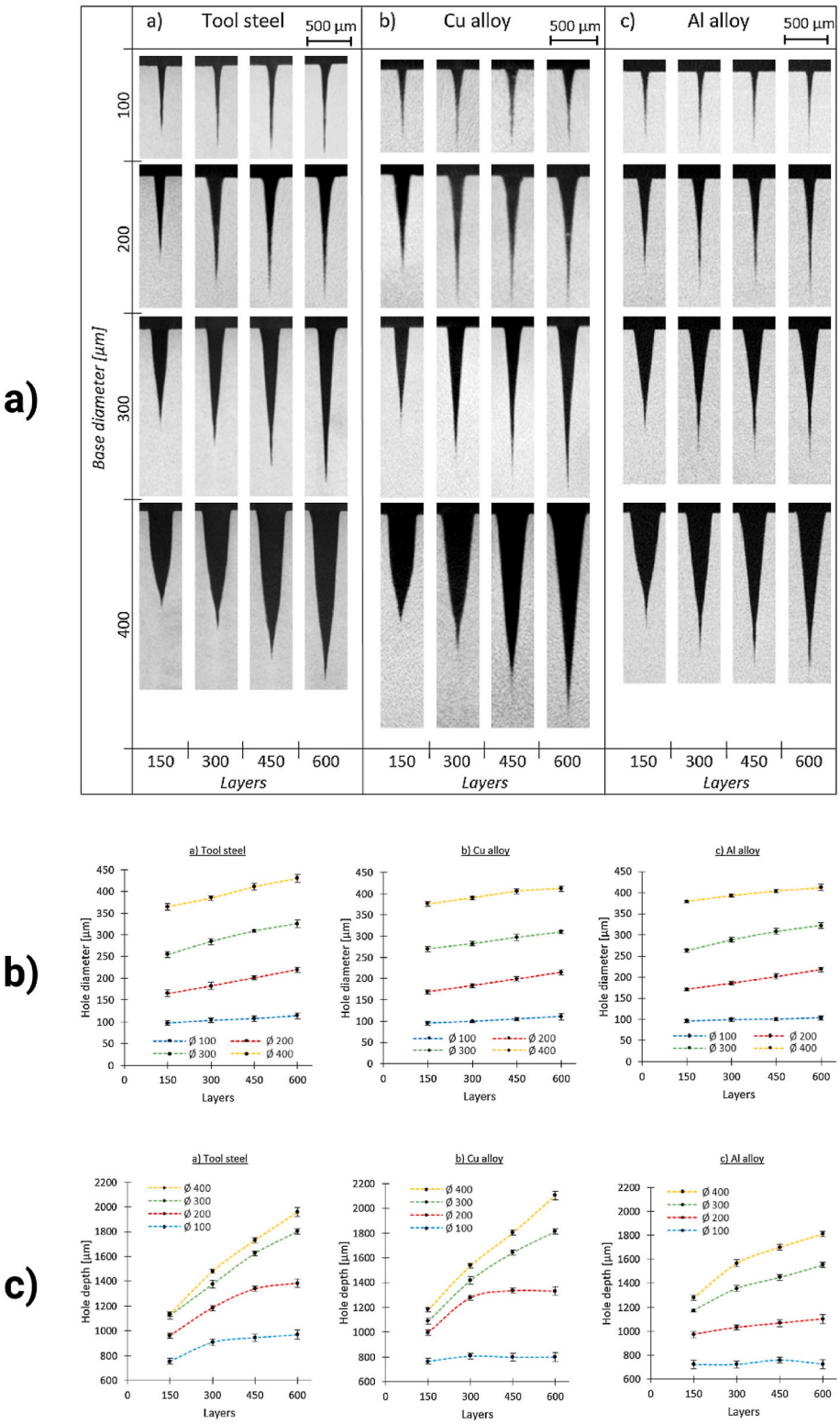

Fig. 13. The geometrical comparison of laser ablated micro-holes per variables, including base diameters (100, 200, 300, and 400 µm), number of laser machining layers (150, 300, 450, and 600) and different mould materials (tool steel, copper alloy, and aluminium alloy). a) Cross-sectional images of micro-cavities in various base diameters and layer numbers. b) A comparison of hole diameter versus the number of layers. c) A comparison of hole depth versus the number of layers. Adapted with permission from Ref. [102], Copyright 2021, Elsevier.

conditions, especially in the case of 150 machining layers caused by the negative dynamic effects of the optical beam deflector system. Furthermore, it is concluded that by increasing the number of layers, the growth rate of hole depth for cases with programmed base diameters of 100 and 200 µm is lower than for cases of 300 and 400 µm, as indicated in Fig. 13c. Overall, as base diameter and layer quantities increase, a higher depth of holes is achieved.

In laser micromachining, the thermal impacts on the ablated

substrate cause alteration of microstructure and mechanical properties, which results in unwanted influences like surface cracking [133,134].

7.2.1.2. Mould fabrication for hollow microneedles replication. Fabrication of mould inserts for manufacturing injected moulded hollow microneedles has been conducted despite its challenges. Yung et al. [127] replaced the two conventional mould inserts with a three-mould-insert system to eliminate the need for the vacuum system. Using a picosecond laser machine, researchers fabricated all mould parts from heat-treated stainless steel with a helical drilling method. In a two-mould insert system, air could be trapped near the tip of the cavity, making the filling and ejection steps difficult, especially for high aspect ratio microneedles. However, the new system allowed the air around the tip area to be vented due to the small gap in the added mould insert. In another study, Evens et al. [17] and Vanwersch et al. [119] used an ultrashort pulse laser ablation method to manufacture cone-shaped hollow microneedle cavities on aluminium zinc alloy and low corrosion tool steel materials, respectively, and evaluated them by μ-CT. The study adopted a cross-hatching laser approach and defined a particular location as the scan-free area (SFA) to specify the internal area of the hollow microneedle. In the SFA position, laser pulses are not transmitted, which ensures that the mould-injected microneedle arrays are hollow. In this layer-by-layer laser ablating strategy, the hatch and layer pitch are characterised as the distance between the parallel lines and layers. The eccentricity parameter is the distance between the centres of SFA and the laser-machined area. This work investigated the influences of laser strategy factors such as base geometry, SFA diameter and location, scanning diameter and number of layers on micro-cavities shape through μ-CT measurements. It was concluded that the effect of SFA diameter on the depth of the cavity is negligible, but a greater SFA area leads to a higher depth of lumen-forming pillar. Also, the results showed that increasing the number of layers increases the depth of the cavity and ridge-forming trench. Nevertheless, the depth-increasing rate was lower for a higher number of layers due to the lower ablation in the deeper parts of the cavity. Evens et al. [102] also concluded a similar outcome about fabricating a negative mould for solid microneedles.

7.2.2. Electroplating and etching

In another method, electroplating and etching techniques are used to fabricate negative metal mould cavities of microneedles with improved surface quality. In the first step, the fabricated microneedles master is polished through electrochemical etching, making it smoother and sharper. Then, the metal negative mould is formed by electroplating on the microneedles master. Izumi et al. [135] manufactured nickel moulds using sharpened silicon microneedles. In their work, after electroplating nickel using a Watts bath solution, the silicon needle master and nickel cavity were etched away.

7.3. Effects of thermoplastic properties on replication process

The physical properties of the thermoplastic polymeric materials influence the replication of microneedles in microinjection moulding. Therefore, studying thermoplastic properties like melt rheology and solidification process is crucial for selecting the optimised polymer. The main parameters, including shrinkage, wettability, viscosity, and creep deformation, are discussed below:

The specific volume of thermoplastic melt during the moulding/cooling step decreases, which causes polymer shrinkage, affecting the final product. Regarding the compressibility of polymers, the specific volume is specified by Evens et al. [102] as a function of the temperature and pressure of the melt, as shown in Equation (1) [102].

$$v(T,P) = v_0 \times \left[1 - 0.0894 \times ln\left(1 + \frac{P}{\beta}\right)\right] + v_T \quad (1)$$

where v_0 is the reference-specific volume, v_T is the extra specific volume related to semi-crystalline polymers, β is the parameter of compressibility, and P is the pressure. Then, the ratio of specific volume at the end of the packing step to the fully cooled product is described in Equation (2).

$$r_v = v\left(T_{no-flow}, P_{pack}\right) / v\left(T_{final}, P_{final}\right) \quad (2)$$

Hence, the linear shrinkage can be estimated through Equation (3). For instance, it is shown that the linear shrinkage of PC microneedles is a few micrometres, while this factor is in the orders of a few tens of micrometres for PP material [102].

$$s = 1 - \sqrt[3]{r_v} \quad (3)$$

The pressure–specific volume–temperature (PvT) diagram is widely recognised and commonly used in the plastics injection moulding industry. Parameters such as injection temperature, holding pressure, holding time, and cooling time all influence the specific volume and shrinkage behaviour of polymers [136]. In a case study, Wang et al. [136] used a PvT testing device to directly measure the specific volume of semi-crystalline PP and amorphous ABS. Their findings showed that the starting temperature, which corresponds to the injection temperature, significantly affects the specific volume during the injection moulding process. Higher starting temperatures result in greater specific volumes. However, the starting temperature has a relatively minor effect on shrinkage, although an increase in this temperature can lead to a slight reduction in shrinkage. Among all the process parameters, holding pressure significantly impacts specific volume and phase transition temperature. Higher holding pressures reduce the specific volume, raise the phase transition temperature, and result in lower shrinkage. The temperature at the end of the holding stage is closely related to the holding time. Lower holding-end temperatures extend the holding time and lead to reduced specific volumes. A longer holding time also allows more free volume within the polymer to diffuse, minimising shrinkage. Furthermore, the specific volume of polymers decreases as the cooling rate is reduced during the shrinkage stage [136].

Another significant factor affecting micro-cavity filling is wettability, defined as the tendency of liquid (molten polymer) to spread on the solid surface (metal mould). This parameter is determined through contact angle and adhesion measurements, which are also influenced by mould surface roughness and the mould and melt temperature. The higher the adhesion, the better the melt fills the mould [137]. For instance, in a study by Vera et al. [138], PP material showed superior replication on a steel mould compared to PC due to the higher adhesion.

Furthermore, the viscosity of molten polymer plays a significant role in filling efficiency. Relative molecular mass, melt pressure, and temperature impact the viscosity of thermoplastics. As the molecular weight decreases, the polymer viscosity drops. The melt viscosity decreases as the shear rate increases, a phenomenon known as shear thinning in non-Newtonian fluids. This occurs because the polymer chains disentangle and align in the flow direction. As a result, higher shear rates reduce melt viscosity, making filling small structures, such as microneedle cavities, easier. Two distinct shear rate conditions can be identified during the micro-cavity filling process. A very high shear rate during the injection phase partially fills the microneedle cavities, and a much lower shear rate during the packing phase helps to further complete the filling [102,139]. The melt viscosity can be extracted from the Cross-WLF model [102,139,140].

Furthermore, thixotropy refers to the rheological characteristic of a material where its viscosity gradually decreases while being subjected to shear over time and then gradually recovers once the shear is removed. This gradual recovery in thixotropic materials allows the melt to continue flowing and complete the filling during the packing phase [141,142]. Increasing injection velocity and pressure raises the shear rate, which enhances shear thinning and improves the melt flow rate (MFR) to fill the small micro-cavities with high aspect ratios. However, excessive injection pressures and speeds can lead to polymer

degradation and early solidification. Holding pressure and time must be precisely managed to ensure complete cavity filling after the initial injection, especially considering viscosity changes caused by thixotropic behaviour. Increasing the mould temperature can also help by slowing the cooling process and maintaining the melt's flowability, although it may also lead to longer cycle times [111,119,143–145].

The other variable which distinguishes different thermoplastics is creep deformation behaviour. When the mould is packed, the polymer boundary layer near the mould surface is under deformation, which helps better filling than the initial step. This deformation can only occur if the temperature of the surface layer remains higher than the no-flow temperature, which is defined as the temperature at which the polymer stops flowing [146,147]. The required time for the polymer to reach the no-flow temperature is calculated by Equation (4) [148]. By using this equation, it is possible to compare the time required for different thermoplastics to reach their no-flow temperature. This comparison can also be applied across various cavity geometries, injection temperatures, and mould temperatures for further optimisations. A shorter time results in faster solidification of the polymer boundary layer near the mould surface, thereby limiting deformation at the start of the packing phase [102]. For instance, Evens et al. [102] demonstrated that this time for the PP material is approximately twice that of the PC material. This indicates that, at the start of packing, the PC near the mould surface may have solidified and lost its ability to deform, while the PP is still undergoing deformation.

$$t = \frac{a^2}{\pi^2 \times \alpha} \times Ln\left[\frac{8}{\pi^2} \times \left(\frac{T_i - T_m}{T_{nf} - T_m}\right)\right] \tag{4}$$

Where a is the thickness of the micropart, α is thermal diffusivity, T_i is the injection temperature, T_m is the mould temperature and T_{nf} is the no-flow temperature.

7.4. Assessment of microneedles quality in mass production approach

In all manufacturing techniques, assessing fabricated microneedles quality is highly significant in inspecting the accuracy of dimensional features and mechanical properties. Image processing, as a popular optical method, has been used for the geometrical evaluation of microneedles using high-resolution microscopes like Scanning Electron Microscope (SEM) [149,150], 3D Laser Scanning Confocal Microscopy (LSCM), and Atomic Force Microscopy (AFM) [128]. Additionally, several *in vivo* or *in vitro* mechanical experiments, including force-displacement and compression tests, are applied to demonstrate the physical parameters such as penetration force, failure force, and insertion depth of microneedles [45,46]. However, assessing large quantities of microneedles fabricated using the injection moulding technique is challenging, as conventional optical methods are time-consuming. Therefore, an accurate and quick strategy is needed to assess the quality of products manufactured in large numbers [151]. Gülçür et al. [16] developed an inspection setup based on telecentric imaging and machine vision in micro-scales, which allowed the evaluation of 36 individual mould-injected microneedles in only 2 min. In their study, a machine vision camera was employed to capture shadow images of microneedles positioned midway along the optical path between the camera and a telecentric backlight illuminator. A 5x telecentric objective lens focused the image onto the camera's sensor, which has a resolution of 5.3 megapixels and operates at a frame rate of 75 Hz. To focus on each of the 36 individual microneedles on the replicas, two translational stages enabled precise movement along the x and y axes. The microneedles were aligned at a 5° angle relative to the axis perpendicular to the main optical axis to calculate the dx and dy values used for the translational stages. This alignment facilitated the accurate positioning of each microneedle along the optical axis for proper imaging and focusing. Edge detection was applied to the 2D images to identify each microneedle's boundary, with the tip defined as the edge point closest to the top border of the image. The microneedle tip coordinates and the substrate baseline were used to calculate the microneedle's height. This imaging technique, which is based on telecentric imaging and machine vision, is well-suited for the quality assessment of mould-injected microneedles, where dimensional tolerances at the micro-scale are critical. Accurate, repeatable, and rapid characterisation of microneedle geometries enables real-time feedback for quality control and process optimisation [16]. This novel quality assessment technique can also be implemented into an in-line monitoring system to evaluate the quality of fabricated microneedles based on the process parameters. Subsequently, the real-time monitoring system will avoid fabricating damaged products in a mass production approach.

8. Challenges of the microinjection moulding process

In injection moulding process as the dimension and volume of the ultimate product decrease to micron size, the fabrication process will be more complicated due to the small size of the mould cavity and desired filling efficiency. Miniaturising the large-scale injection moulding machine is ineffective in acquiring the desired products. Scaling down the procedure affects the final product's properties, replication accuracy, geometry, structure, and mechanical strength. Therefore, it is essential to understand and optimise the micro features and factors of different components and steps of the microinjection moulding process to secure the quality of final products. The quality of the surface, edge definition, and material rheology are affected by main design factors, including the molten polymer and mould temperature, injection velocity and pressure, injection time, cooling time, and clamping force [145,152].

In the microinjection moulding method, accurately adjusting a small amount of molten polymeric material and the injection speed is challenging [153]. The volumetric injection rate impacts the efficiency of filling the micro-cavities. As the volume of melt injection increases, the injection time decreases, which postpones the solidification of prior polymeric layers [94,154]. However, there is a limitation to the maximum injection flow rate due to the possibility of polymer degradation caused by shear stress. Subsequently, the size and the movement of the screw or plunger should be in scales of millimetres and micrometres, respectively [87].

Moreover, designing a demoulding system that applies an optimised ejection force on micro-scale products at the end of each cycle without any imperfections is highly significant. An adequate force is required for demoulding to control the shear stresses caused by friction between the surface of the mould and the finished product [155]. Precision electropolishing has been employed as a shaping and polishing method to optimise the fillet radius of features, facilitating smoother demoulding [156]. The holding pressure plays a significant role in filling the cavities by force to overcome the polymer shrinkage problem, which leads to a favourable shape formation [154]. Also, the switch-over pressure plays a crucial role in the filling efficiency of mould cavities, which governs the transition from the injection step to the packing process. As the switch-over pressure increases, the injection piston decelerates slightly later, and more molten material is injected, resulting in greater packing and fabrication performance [16].

Furthermore, due to the high ratio of surface to volume, when the melted material reaches the low-temperature surface of the mould, the solidification process will take place earlier. This will avoid filling the entire cavity, particularly in cases with greater aspect ratios. Another challenge is the hesitation effect that the molten material tends to flow through parts of the mould cavity with a higher thickness and lower resistance. Accordingly, compared with large-scale injection moulding, the pressure, velocity and temperature of melt and mould should be raised to the highest possible value to provide quick filling and overcome premature cooling [143,155]. However, there are some restrictions in increasing these parameters; for instance, polymer degradation is caused by higher melt temperatures and injection pressures [111]. It happens due to the friction between layers of

thermoplastic flowing within the mould cavity. Excessive shear stress can lead to plastic degradation and failure through stress cracking. In addition, as mould temperature increases, the time and cost of the cooling process rise, leading to longer cycle times [145]. Overall, to prevent some undesirable features such as product defects caused by the incomplete injection, existence of flash, material waste, long cycle time, residual polymer (from the prior cycle) in the injection unit, and thermal degradation of the polymer, all of the design factors should be optimised simultaneously to ensure a reliable replication procedure and to overcome technological restrictions.

Various studies were conducted to assess the effects of microinjection moulding variables on fabrication precision. Packianather et al. [157] investigated the influences of microinjection moulding parameters, including barrel temperature, mould temperature, holding pressure, and injection speed, on the replication process experimentally. The work aimed to optimise the injection factors to determine the specific amount of ejection force. The comparison of parameters interaction showed that mould temperature and holding pressure are the most effective factors. Mani et al. [144] studied the effects of injection speed, injection pressure, and the temperature of molten material on the accuracy of microchannel dimensions. The experiments used two materials, polyoxymethylene (POM) and liquid crystal polymer (LCP), indicating that higher pressure and temperature of injected melt make a more precise product. However, these increments will cause greater flash on the finished part. Flash is a defect when the melt leaks from the mould during injection and solidification. The cooling rate also significantly influences the product's internal structure and mechanical properties. Babenko et al. [158] conducted experiments to determine the influence of heat flux and cooling curves. Moreover, they conducted numerical simulations using Moldflow software to determine the heat transfer coefficient that fitted the cooling curves. It was observed that the most appropriate heat transfer coefficient of the mould/melt interface is 7700 $W/m^2\,^{\circ}C$ to model the experimental results. Bellantone et al. [159] investigated the influence of microinjection parameters on the quality and mass of a bone-shaped sample made with POM and LCP. The results illustrated that for POM, holding pressure and holding time have the most impact on the mass of the product. On the other hand, in the case of LCP, the two factors of holding pressure and injection velocity are the most influential parameters for obtaining higher part mass. Furthermore, melt compressibility significantly influences the weight of the microparts. The results showed how much a material can be compacted under pressure, directly affecting the fabricated micropart's final density and mass [160]. Trotta et al. [139] analysed the rheology of the molten polymer in a cavity with various thicknesses using a microinjection machine consisting of pressure and temperature sensors. According to the results, by increasing injection velocity and pressure, the lower viscosity of the melt dominates filling obstacles and improves fabrication efficiency. The trapped air pressure inside the mould cavity also caused polymer gasification and resistance in front of the melt during the injection step, leading to incomplete polymer filling. It may further affect the mass of the microparts by forming voids within the material, which leads to variations in density and mass, as well as potential structural weaknesses. Therefore, air removal utilising a vacuum system is a highly effective solution to ensure a uniform mass and improve the dimensional micro-features, particularly on edges. Meanwhile, by air evacuation, the temperature of the mould decreases. Sorgato et al. [161] concluded that the temperature gradient of mould and molten material is influenced by vacuum venting. Yu et al. [106] manufactured in-plane PLA microneedles through the microinjection moulding method and numerically studied the effects of the combination of process parameters on "filling fraction", defined as the ratio of the filled material to the total volume of mould cavities. It was observed that as the injection time increased, the filling efficiency decreased. For instance, the worst case was related to an injection time of 6 s with a filling fraction of 66.21 %. Moreover, the mould was thoroughly filled when the melt temperature was 220 °C or 230 °C. It was also concluded that an increase in packing pressure leads to higher filling fractions, and the parameter of packing time is irrelevant.

9. Conclusion and future outlook

Developing a cost-effective and rapid method for producing microneedles in large quantities is essential due to the rapid development of microneedle technologies and their advantages for clinical applications [162,163]. When comparing microneedle materials, biocompatible polymers are increasingly favoured for mass production due to their affordability, satisfactory mechanical properties, biodegradability, and excellent chemical stability. Among all manufacturing techniques used to fabricate polymeric microneedles, microinjection moulding offers substantial potential for mass production of micron-sized needles. The injection moulding technique yields higher product quantities in a shorter duration due to the faster cycle time and reduced microinjection moulding machine assembly steps.

The injection moulding fabrication process, machine operations, technological advancements, and the fabrication challenges of microneedles, were discussed in detail. Solid and hollow microneedles have primarily been manufactured using the microinjection moulding technique. In addition, some post-processing techniques, such as piezoelectric inkjet coating and dip-coating, have been utilised for drug deposition on microinjected solid microneedles to make coated microneedles. Microinjection moulding machines used for fabricating microneedles are categorised into conventional and ultrasonic types, distinguished by their plasticisation mechanisms. It is specified that ultrasonic microinjection machines demonstrate greater efficiency in energy consumption and material savings.

In addition to scaling down and modifying the machine, it is crucial to optimise design parameters such as mould and melt temperatures, injection speed and pressure, packing pressure, and volumetric injection rate. These factors significantly impact the quality of the final desired shape. As the most significant factor, higher mould temperatures allow molten materials to fill the micro-cavities more effectively; however, this variable has an upper limit due to heat deflection issues during demoulding and increased cycle time. It is also concluded that increasing the injection pressure enhances filling efficiency and results in sharper microneedles' tips. Nonetheless, the maximum value of this parameter is restricted to avoid polymer degradation that occurs in high shear stresses.

As the desired product volume decreases to micron size, the manufacturing process becomes challenging due to potential issues such as premature solidification and hesitation effects in micro-cavities. It is determined that in double-step micro-machines, an injection plunger with a few millimetres in diameter enables a more accurate dose of injected melt at higher injection speeds, which improves the filling efficiency for the fabrication of microneedles.

Given the significant role of mould manufacturing in accurately shaping microneedles during the microinjection moulding process, this review also discussed the metal mould fabrication process and its challenges. Laser micromachining, as a subtractive technique, is predominantly utilised to fabricate negative metal moulds of microneedles. This manufacturing method makes it highly challenging to form microcavities with complicated geometries, particularly with extremely low tip radius due to the plasma shielding effect and laser reflectance problems. Furthermore, the mould fabrication process for hollow microneedles is complicated and time-consuming, and mould inserts must be modified. Also, layer-by-layer laser ablation is primarily suitable for metals with higher electron-phonon coupling constants and thermal conductivity. Laser thermal effects may cause some undesirable influences on the mechanical properties of the metal mould, such as surface cracking. According to the limitations and challenges of laser micromachining on a micro-scale, replacing this subtractive method with a more efficient technique like additive manufacturing is

beneficial. It provides the opportunity to fabricate more complicated geometries and overcome current drawbacks.

The physical and rheological properties of thermoplastic polymers affect the quality of microneedles in microinjection moulding. Biocompatible polymers with low shrinkage, high wettability and flowability, superior mechanical properties, and low melt viscosity are highly desirable. Despite the current developments, further developments in the microinjection moulding of microneedles with biocompatible thermoplastic polymers are required.

CRediT authorship contribution statement

Pouria Azarikhah: Writing – review & editing, Writing – original draft, Visualization, Validation, Software, Methodology, Investigation, Formal analysis, Data curation, Conceptualization. **Asim Mushtaq:** Writing – review & editing, Visualization, Software, Methodology, Conceptualization. **Khaled Mohammed Saifullah:** Writing – review & editing, Visualization, Software, Investigation, Conceptualization. **Philip D. Prewett:** Writing – review & editing, Supervision, Methodology, Investigation, Conceptualization. **Graham J. Davies:** Writing – review & editing, Supervision, Methodology, Investigation, Conceptualization. **Zahra Faraji Rad:** Writing – review & editing, Validation, Supervision, Resources, Project administration, Methodology, Investigation, Formal analysis, Data curation, Conceptualization.

Statements and declarations

The authors declare that they have no financial interests or personal relationships that could have influenced the work presented in this paper.

Ethical standards

The manuscript does not contain clinical studies or patient data.

Declaration of competing interest

The authors declare that they have no known competing financial interests or personal relationships that could have appeared to influence the work reported in this paper.

List of Abbreviations

SC	Stratum Corneum
TDD	Transdermal Drug Delivery
FDM	Fused Deposition Modelling
TPP	Two-photon Polymerisation
HF	Hydrogel-Forming
ISF	Interstitial Fluid
PVA	Polyvinyl Alcohol
PVP	Polyvinylpyrrolidone
PC	Polycarbonate
PP	Polypropylene
PMMA	Poly Methyl Methacrylate
PLA	Polylactic Acid
PLGA	Poly Lactic-co-Glycolic Acid
GelMA	Gelatin Methacryloyl
MEMS	Microelectromechanical Systems
MST	Microsystems
COC	Cyclic Olefin Copolymers
COP	Cyclic Olefin Polymer
PS	Polystyrene
PE	Polyethylene
POM	Polyoxymethylene
LCP	Liquid Crystal Polymer
LLDPE	Linear Low-density Polyethylene
ABS	Acrylonitrile Butadiene Styrene
PET	Polyethylene Terephthalate
PGA	Polyglycolic Acid
PEEK	Polyether Ether Ketone
PPDO	Poly(p-dioxanone)
PDMS	Polydimethylsiloxane
μ-EDM	Micro-Electrical Discharge Machining
NC	Numerical Control
LIGA	Lithography, Electroplating, and Moulding
pHEMA	2-Hydroxyethylmethacrylate
μ-CT	Micro-Computed Tomography
SFA	Scan-Free-Area
MFR	Melt Flow Rate
SEM	Scanning Electron Microscope
LSCM	Laser Scanning Confocal Microscopy
AFM	Atomic Force Microscopy

Appendix A. Supplementary data

Supplementary data to this article can be found online at https://doi.org/10.1016/j.jddst.2025.107435.

Data availability

Data will be made available on request.

References

[1] Y.-C. Kim, J.-H. Park, M.R. Prausnitz, Microneedles for drug and vaccine delivery, Adv. Drug Deliv. Rev. 64 (14) (2012) 1547–1568, https://doi.org/10.1016/j.addr.2012.04.005.

[2] R.K. Sivamani, D. Liepmann, H.I. Maibach, Microneedles and transdermal applications, Expet Opin. Drug Deliv. 4 (1) (2007) 19–25, https://doi.org/10.1517/17425247.4.1.19.

[3] Z. Faraji Rad, R.E. Nordon, G.J. Davies, C.J. Anthony, P. Prewett, Microfluidic devices and fabrication, U.S. Patent (2020) 15508519, 10850082.

[4] K. Ita, Transdermal delivery of drugs with Microneedles—potential and challenges, Pharmaceutics 7 (3) (2015) 90–105, https://doi.org/10.3390/pharmaceutics7030090.

[5] M.B. Brown, A.C. Williams, The Art and Science of Dermal Formulation Development, CRC Press, 2019, https://doi.org/10.1201/9780429059872.

[6] J.J. Escobar-Chávez, D. Bonilla-Martínez, M. Angélica, E. Molina-Trinidad, N. Casas-Alancaster, A.L. Revilla-Vázquez, Microneedles: a valuable physical enhancer to increase transdermal drug delivery, J. Clin. Pharmacol. 51 (7) (2011) 964–977, https://doi.org/10.1177/0091270010378859.

[7] R.F. Donnelly, T.R.R. Singh, D.I. Morrow, A.D. Woolfson, Microneedle-Mediated Transdermal and Intradermal Drug Delivery, John Wiley & Sons, Hoboken, NJ, USA, 2012.

[8] T. Waghule, G. Singhvi, S.K. Dubey, M.M. Pandey, G. Gupta, M. Singh, K. Dua, Microneedles: a smart approach and increasing potential for transdermal drug delivery system, Biomed. Pharmacother. 109 (2019) 1249–1258, https://doi.org/10.1016/j.biopha.2018.10.078.

[9] K.M. Kwon, S.-M. Lim, S. Choi, D.-H. Kim, H.-E. Jin, G. Jee, K.-J. Hong, J.Y. Kim, Microneedles: quick and easy delivery methods of vaccines, Clin. Experim. Vaccine Res. 6 (2) (2017) 156–159, https://doi.org/10.7774/cevr.2017.6.2.156.

[10] H. Suh, J. Shin, Y.-C. Kim, Microneedle patches for vaccine delivery, Clin. Experim. Vaccine Res. 3 (1) (2014) 42–49, https://doi.org/10.7774/cevr.2014.3.1.42.

[11] K.M. Saifullah, Z. Faraji Rad, Sampling dermal interstitial fluid using microneedles: a review of recent developments in sampling methods and microneedle-based biosensors, Adv. Mater. Interfac. 10 (10) (2023) 2201763, https://doi.org/10.1002/admi.202201763.

[12] L.K. Vora, A.H. Sabri, P.E. McKenna, A. Himawan, A.R. Hutton, U. Detamornrat, A.J. Paredes, E. Larrañeta, R.F. Donnelly, Microneedle-based biosensing, Nat. Rev. Bioeng. 2 (1) (2024) 64–81, https://doi.org/10.1038/s44222-024-00223-z.

[13] K.M. Saifullah, P. Azarikhah, Z. Faraji Rad, Synthesis-free swellable hydrogel microneedles for rapid interstitial fluid extraction and on-site glucose detection via an electrochemical biosensor system, Mater. Today Chem. 45 (2025) 102661, https://doi.org/10.1016/j.mtchem.2025.102661.

[14] K.M. Saifullah, A. Mushtaq, P. Azarikhah, P.D. Prewett, G.J. Davies, Z. Faraji Rad, Micro-vibration assisted dual-layer spiral microneedles to rapidly extract dermal interstitial fluid for minimally invasive detection of glucose, Microsys. Nanoeng. 11 (1) (2025) 3, https://doi.org/10.1038/s41378-024-00850-x.

[15] D. Sil, S. Bhowmik, P. Patel, B.D. Kurmi, Promising role of microneedles in therapeutic and biomedical applications, J. Drug Deliv. Sci. Technol. 91 (2024) 105273, https://doi.org/10.1016/j.jddst.2023.105273.

[16] M. Gülçür, J.-M. Romano, P. Penchev, T. Gough, E. Brown, S. Dimov, B. Whiteside, A cost-effective process chain for thermoplastic microneedle manufacture combining laser micro-machining and micro-injection moulding, CIRP J. Manuf. Sci. Technol. 32 (2021) 311–321, https://doi.org/10.1016/j.cirpj.2021.01.015.

[17] T. Evens, L. Van Hileghem, F. Dal Dosso, J. Lammertyn, O. Malek, S. Castagne, D. Seveno, A. Van Bael, Producing hollow polymer microneedles using laser ablated molds in an injection molding process, J. Micro Nano-Manufact. 9 (3) (2021) 030902, https://doi.org/10.1115/1.4051456.

[18] X. Jin, D.D. Zhu, B.Z. Chen, M. Ashfaq, X.D. Guo, Insulin delivery systems combined with microneedle technology, Adv. Drug Deliv. Rev. 127 (2018) 119–137, https://doi.org/10.1016/j.addr.2018.03.011.

[19] R. Nagarkar, M. Singh, H.X. Nguyen, S. Jonnalagadda, A review of recent advances in microneedle technology for transdermal drug delivery, J. Drug Deliv. Sci. Technol. 59 (2020) 101923, https://doi.org/10.1016/j.jddst.2020.101923.

[20] T. Evens, O. Malek, S. Castagne, D. Seveno, A. Van Bael, A novel method for producing solid polymer microneedles using laser ablated moulds in an injection moulding process, Manufactut. Lett. 24 (2020) 29–32, https://doi.org/10.1016/j.mfglet.2020.03.009.

[21] J.M. Lippmann, E.J. Geiger, A.P. Pisano, Polymer investment molding: method for fabricating hollow, microscale parts, Sensor Actuator Phys. 134 (1) (2007) 2–10, https://doi.org/10.1016/j.sna.2006.05.009.

[22] M.S. Lhernould, M. Deleers, A. Delchambre, Hollow polymer microneedles array resistance and insertion tests, Int. J. Pharm. 480 (1–2) (2015) 152–157, https://doi.org/10.1016/j.ijpharm.2015.01.019.

[23] Y. Li, H. Zhang, R. Yang, Y. Laffitte, U. Schmill, W. Hu, M. Kaddoura, E. J. Blondeel, B. Cui, Fabrication of sharp silicon hollow microneedles by deep-reactive ion etching towards minimally invasive diagnostics, Microsys. Nanoeng. 5 (1) (2019) 41, https://doi.org/10.1038/s41378-019-0077-y.

[24] C. O'Mahony, A. Bocchino, M.J. Haslinger, S. Brandstätter, H. Außerhuber, K. Schossleitner, A.J.P. Clover, D. Fechtig, Piezoelectric inkjet coating of injection moulded, reservoir-tipped microneedle arrays for transdermal delivery, JMiMi 29 (8) (2019) 085004, https://doi.org/10.1088/1361-6439/ab222b.

[25] Y. Mizuno, K. Takasawa, T. Hanada, K. Nakamura, K. Yamada, H. Tsubaki, M. Hara, Y. Tashiro, M. Matsuo, T. Ito, Fabrication of novel-shaped microneedles to overcome the disadvantages of solid microneedles for the transdermal delivery of insulin, Biomed. Microdevices 23 (2021) 1–8, https://doi.org/10.1007/s10544-021-00576-x.

[26] J.-H. Park, M.G. Allen, M.R. Prausnitz, Biodegradable polymer microneedles: fabrication, mechanics and transdermal drug delivery, J. Contr. Release 104 (1) (2005) 51–66, https://doi.org/10.1016/j.jconrel.2005.02.002.

[27] Y. Zhang, K. Brown, K. Siebenaler, A. Determan, D. Dohmeier, K. Hansen, Development of lidocaine-coated microneedle product for rapid, safe, and prolonged local analgesic action, Pharm. Res. 29 (2012) 170–177, https://doi.org/10.1007/s11095-011-0524-4.

[28] Y. Zhang, K. Siebenaler, K. Brown, D. Dohmeier, K. Hansen, Adjuvants to prolong the local anesthetic effects of coated microneedle products, Int. J. Pharm. 439 (1–2) (2012) 187–192, https://doi.org/10.1016/j.ijpharm.2012.09.041.

[29] K. Nair, B. Whiteside, C. Grant, R. Patel, C. Tuinea-Bobe, K. Norris, A. Paradkar, Investigation of plasma treatment on micro-injection moulded microneedle for drug delivery, Pharmaceutics 7 (4) (2015) 471–485, https://doi.org/10.3390/pharmaceutics7040471.

[30] X. Jiang, W. Zhang, R. Terry, W. Li, The progress of fabrication designs of polymeric microneedles and related biomedical applications, BMEMat 1 (4) (2023) e12044, https://doi.org/10.1002/bmm2.12044.

[31] A. Sachan, R.J. Sachan, J. Lu, H. Sun, Y.J. Jin, D. Erdmann, J.Y. Zhang, R. J. Narayan, Injection molding for manufacturing of solid poly (l-lactide-co-glycolide) microneedles, MRS Adv. 6 (2021) 61–65, https://doi.org/10.1557/s43580-021-00030-3.

[32] Clarivate web of science. www.webofscience.com. (Accessed 7 August 2025).

[33] M. Azmana, S. Mahmood, A.R. Hilles, U.K. Mandal, K.A.S. Al-Japairai, S. Raman, Transdermal drug delivery system through polymeric microneedle: a recent update, J. Drug Deliv. Sci. Technol. 60 (2020) 101877, https://doi.org/10.1016/j.jddst.2020.101877.

[34] J. Ju, C.-M. Hsieh, Y. Tian, J. Kang, R. Chia, H. Chang, Y. Bai, C. Xu, X. Wang, Q. Liu, Surface enhanced Raman spectroscopy based biosensor with a microneedle array for minimally invasive in vivo glucose measurements, ACS Sens. 5 (6) (2020) 1777–1785, https://doi.org/10.1021/acssensors.0c00444.

[35] N.G. Oh, S.Y. Hwang, Y.H. Na, Fabrication of a PVA-Based hydrogel microneedle patch, ACS Omega 7 (29) (2022) 25179–25185, https://doi.org/10.1021/acsomega.2c01993.

[36] K.N. Mangang, P. Thakran, J. Halder, K.S. Yadav, G. Ghosh, D. Pradhan, G. Rath, V.K. Rai, PVP-microneedle array for drug delivery: mechanical insight, biodegradation, and recent advances, J. Biomater. Sci. Polym. Ed. 34 (7) (2023) 986–1017, https://doi.org/10.1080/09205063.2022.2155778.

[37] H.X. Nguyen, A.K. Banga, Delivery of methotrexate and characterization of skin treated by fabricated PLGA microneedles and fractional ablative laser, Pharm. Res. 35 (2018) 1–20, https://doi.org/10.1007/s11095-018-2369-6.

[38] Z. Luo, W. Sun, J. Fang, K. Lee, S. Li, Z. Gu, M.R. Dokmeci, A. Khademhosseini, Biodegradable gelatin methacryloyl microneedles for transdermal drug delivery, Adv. Healthcare Mater. 8 (3) (2019) 1801054, https://doi.org/10.1002/adhm.201801054.

[39] C. Radhika, B. Gnanavel, Finite element analysis of polymer microneedle for transdermal drug delivery, Mater. Today Proc. 39 (2021) 1538–1542, https://doi.org/10.1016/j.matpr.2020.05.549.

[40] L. Pan, W. Wu, J. Liu, X. Li, Ultrasonic plasticization microinjection precision molding of Polypropylene microneedle arrays, ACS Appl. Polym. Mater. 5 (11) (2023) 9354–9363, https://doi.org/10.1021/acsapm.3c01844.

[41] J.W. Lee, M.-R. Han, J.-H. Park, Polymer microneedles for transdermal drug delivery, J. Drug Target. 21 (3) (2013) 211–223, https://doi.org/10.3109/1061186X.2012.741136.

[42] F. Damiri, N. Kommineni, S.O. Ebhodaghe, R. Bulusu, V.G.S. Jyothi, A.A. Sayed, A.A. Awaji, M.O. Germoush, H.S. Al-Malky, M.Z. Nasrullah, Microneedle-based natural polysaccharide for drug delivery systems (DDS): progress and challenges, Pharmaceuticals 15 (2) (2022) 190, https://doi.org/10.3390/ph15020190.

[43] S. Mdanda, P. Ubanako, P.P. Kondiah, P. Kumar, Y.E. Choonara, Recent advances in microneedle platforms for transdermal drug delivery technologies, Polymers 13 (15) (2021) 2405, https://doi.org/10.3390/polym13152405.

[44] E.M. Cahill, E.D. O'Cearbhaill, Toward biofunctional microneedles for stimulus responsive drug delivery, Bioconjug. Chem. 26 (7) (2015) 1289–1296, https://doi.org/10.1021/acs.bioconjchem.5b00211.

[45] R.X. Liu, Y.T. He, L. Liang, L.F. Hu, Y. Liu, R.X. Yu, B.Z. Chen, Y. Cui, X.D. Guo, Mechanical evaluation of polymer microneedles for transdermal drug delivery: in vitro and in vivo, J. Ind. Eng. Chem. 114 (2022) 181–189, https://doi.org/10.1016/j.jiec.2022.07.008.

[46] G. Bonfante, H. Lee, L. Bao, J. Park, N. Takama, B. Kim, Comparison of polymers to enhance mechanical properties of microneedles for bio-medical applications, Micro and Nano Systems Letters 8 (1) (2020) 1–13, https://doi.org/10.1186/s40486-020-00113-0.

[47] J.-H. Park, M.R. Prausnitz, Analysis of mechanical failure of polymer microneedles by axial force, J. Kor. Phys. Soc. 56 (4) (2010) 1223, https://doi.org/10.3938/jkps.56.1223.

[48] X. Hong, L. Wei, F. Wu, Z. Wu, L. Chen, Z. Liu, W. Yuan, Dissolving and biodegradable microneedle technologies for transdermal sustained delivery of

drug and vaccine, Drug Des. Dev. Ther. (2013) 945–952, https://doi.org/10.2147/DDDT.S44401.
[49] Z. Faraji Rad, P.D. Prewett, G.J. Davies, An overview of microneedle applications, materials, and fabrication methods, Beilstein J. Nanotechnol. 12 (1) (2021) 1034–1046, https://doi.org/10.3762/bjnano.12.77.
[50] F.K. Aldawood, A. Andar, S. Desai, A comprehensive review of microneedles: types, materials, processes, characterizations and applications, Polymers 13 (16) (2021) 2815, https://doi.org/10.3390/polym13162815.
[51] E. Larrañeta, R.E. Lutton, A.D. Woolfson, R.F. Donnelly, Microneedle arrays as transdermal and intradermal drug delivery systems: materials science, manufacture and commercial development, Mater. Sci. Eng. R Rep. 104 (2016) 1–32, https://doi.org/10.1016/j.mser.2016.03.001.
[52] O. Howells, G.J. Blayney, B. Gualeni, J.C. Birchall, P.F. Eng, H. Ashraf, S. Sharma, O.J. Guy, Design, fabrication, and characterisation of a silicon microneedle array for transdermal therapeutic delivery using a single step wet etch process, Eur. J. Pharm. Biopharm. 171 (2022) 19–28, https://doi.org/10.1016/j.ejpb.2021.06.005.
[53] S. Olhero, E. Lopes, J. Ferreira, Fabrication of ceramic microneedles–the role of specific interactions between processing additives and the surface of oxide particles in epoxy gel casting, J. Eur. Ceram. Soc. 36 (16) (2016) 4131–4140, https://doi.org/10.1016/j.jeurceramsoc.2016.06.035.
[54] R.S. Bhadale, V.Y. Londhe, A systematic review of carbohydrate-based microneedles: current status and future prospects, J. Mater. Sci. Mater. Med. 32 (8) (2021) 89, https://doi.org/10.1007/s10856-021-06559-x.
[55] E.Z. Loizidou, N.T. Inoue, J. Ashton-Barnett, D.A. Barrow, C.J. Allender, Evaluation of geometrical effects of microneedles on skin penetration by CT scan and finite element analysis, Eur. J. Pharm. Biopharm. 107 (2016) 1–6, https://doi.org/10.1016/j.ejpb.2016.06.023.
[56] P. Azarikhah, K.M. Saifullah, Z. Faraji Rad, Age-dependent finite element analysis of microneedle penetration into human skin: influence of insertion velocity, and microneedle's geometry and material, Macromol. Mater. Eng. (2025) e00123, https://doi.org/10.1002/mame.202500123.
[57] A.H. Sabri, Y. Kim, M. Marlow, D.J. Scurr, J. Segal, A.K. Banga, L. Kagan, J.B. Lee, Intradermal and transdermal drug delivery using microneedles–Fabrication, performance evaluation and application to lymphatic delivery, Adv. Drug Deliv. Rev. 153 (2020) 195–215, https://doi.org/10.1016/j.addr.2019.10.004.
[58] J.W. Lee, J.-H. Park, M.R. Prausnitz, Dissolving microneedles for transdermal drug delivery, Biomaterials 29 (13) (2008) 2113–2124, https://doi.org/10.1016/j.biomaterials.2007.12.048.
[59] O. Olatunji, D.B. Das, M.J. Garland, L. Belaid, R.F. Donnelly, Influence of array interspacing on the force required for successful microneedle skin penetration: theoretical and practical approaches, J. Pharm. Sci. 102 (4) (2013) 1209–1221, https://doi.org/10.1002/jps.23439.
[60] L.Y. Chu, M.R. Prausnitz, Separable arrowhead microneedles, J. Contr. Release 149 (3) (2011) 242–249, https://doi.org/10.1016/j.jconrel.2010.10.033.
[61] A.R. Johnson, C.L. Caudill, J.R. Tumbleston, C.J. Bloomquist, K.A. Moga, A. Ermoshkin, D. Shirvanyants, S.J. Mecham, J.C. Luft, J.M. DeSimone, Single-step fabrication of computationally designed microneedles by continuous liquid interface production, PLoS One 11 (9) (2016) e0162518, https://doi.org/10.1371/journal.pone.0162518.
[62] K. Badnikar, S.N. Jayadevi, S. Pahal, S. Sripada, M.M. Nayak, P.K. Vemula, D. N. Subrahmanyam, Generic molding platform for simple, low-cost fabrication of polymeric microneedles, Macromol. Mater. Eng. 305 (5) (2020) 2000072, https://doi.org/10.1002/mame.202000072.
[63] F.K. Aldawood, S. Desai, S.K. Parupelli, A. Andar, Polymeric microneedles using additive manufacturing for therapeutic applications, in: IIE Annual Conference. Proceedings, Institute of Industrial and Systems Engineers (IISE), 2023.
[64] Z. Faraji Rad, R.E. Nordon, C.J. Anthony, L. Bilston, P.D. Prewett, J.-Y. Arns, C. H. Arns, L. Zhang, G.J. Davies, High-fidelity replication of thermoplastic microneedles with open microfluidic channels, Microsys. Nanoeng. 3 (1) (2017) 1–11, https://doi.org/10.1038/micronano.2017.34.
[65] P. Janphuang, M. Laebua, C. Sriphung, P. Taweewat, A. Sirichalarmkul, K. Sukjantha, N. Promsawat, P. Leuasoongnoen, S. Suphachiaraphan, K. Phimol, Polymer based microneedle patch fabricated using microinjection moulding, in: MATEC Web of Conferences, EDP Sciences, 2018, https://doi.org/10.1051/matecconf/201819201039.
[66] T.E. Andersen, A.J. Andersen, R.S. Petersen, L.H. Nielsen, S.S. Keller, Drug loaded biodegradable polymer microneedles fabricated by hot embossing, Microelectron. Eng. 195 (2018) 57–61, https://doi.org/10.1016/j.mee.2018.03.024.
[67] S. Yang, Y. Feng, L. Zhang, N. Chen, W. Yuan, T. Jin, A scalable fabrication process of polymer microneedles, Int. J. Nanomed. (2012) 1415–1422, https://doi.org/10.2147/IJN.S28511.
[68] M.A. Luzuriaga, D.R. Berry, J.C. Reagan, R.A. Smaldone, J.J. Gassensmith, Biodegradable 3D printed polymer microneedles for transdermal drug delivery, LChip 18 (8) (2018) 1223–1230, https://doi.org/10.1039/C8LC00098K.
[69] L. Wu, J. Park, Y. Kamaki, B. Kim, Optimization of the fused deposition modeling-based fabrication process for polylactic acid microneedles, Microsys. Nanoeng. 7 (1) (2021) 58, https://doi.org/10.1038/s41378-021-00284-9.
[70] M.J. Uddin, N. Scoutaris, P. Klepetsanis, B. Chowdhry, M.R. Prausnitz, D. Douroumis, Inkjet printing of transdermal microneedles for the delivery of anticancer agents, Int. J. Pharm. 494 (2) (2015) 593–602, https://doi.org/10.1016/j.ijpharm.2015.01.038.
[71] Z. Faraji Rad, P.D. Prewett, G.J. Davies, High-resolution two-photon polymerization: the Most versatile technique for the fabrication of microneedle arrays, Microsys. Nanoeng. 7 (1) (2021) 71, https://doi.org/10.1038/s41378-021-00298-3.
[72] K. Lee, H.C. Lee, D.S. Lee, H. Jung, Drawing lithography: three-dimensional fabrication of an ultrahigh-aspect-ratio microneedle, Adv. Mater. 22 (4) (2010) 483–486, https://doi.org/10.1002/adma.201090004.
[73] H. Juster, B. van der Aar, H. de Brouwer, A review on microfabrication of thermoplastic polymer-based microneedle arrays, Polym. Eng. Sci. 59 (5) (2019) 877–890, https://doi.org/10.1002/pen.25078.
[74] J.-M. Romano, M. Gulcur, A. Garcia-Giron, E. Martinez-Solanas, B.R. Whiteside, S.S. Dimov, Mechanical durability of hydrophobic surfaces fabricated by injection moulding of laser-induced textures, Appl. Surf. Sci. 476 (2019) 850–860, https://doi.org/10.1016/j.apsusc.2019.01.162.
[75] M. Franchetti, C. Kress, An economic analysis comparing the cost feasibility of replacing injection molding processes with emerging additive manufacturing techniques, Int. J. Adv. Des. Manuf. Technol. 88 (2017) 2573–2579, https://doi.org/10.1007/s00170-016-8968-7.
[76] J. Faludi, N. Cline-Thomas, S. Agrawala, Chapter 5—3D printing and its environmental implications, The next Production Revolution Implications for Governments and Business, Organization for Economic Cooperation and Development (OECD), OECD Publishing, Paris, France, 2017.
[77] J. Zhou, Digitalization and intelligentization of manufacturing industry, Adv. Manufact. 1 (1) (2013) 1–7, https://doi.org/10.1007/s40436-013-0006-5.
[78] R. Farooque, M. Asjad, S. Rizvi, A current state of art applied to injection moulding manufacturing process–a review, Mater. Today Proc. 43 (2021) 441–446, https://doi.org/10.1016/j.matpr.2020.11.967.
[79] G. Singh, A. Verma, A brief review on injection moulding manufacturing process, Mater. Today Proc. 4 (2) (2017) 1423–1433, https://doi.org/10.1016/j.matpr.2017.01.164.
[80] S.M. Mukras, Experimental-based optimization of injection molding process parameters for short product cycle time, Adv. Polym. Technol. 2020 (2020) 1–15, https://doi.org/10.1155/2020/1309209.
[81] P. Pierleoni, L. Palma, A. Belli, L. Sabbatini, Using plastic injection moulding machine process parameters for predictive maintenance purposes, in: 2020 International Conference on Intelligent Engineering and Management (ICIEM), IEEE, 2020, https://doi.org/10.1109/ICIEM48762.2020.9160120.
[82] V. Goodship, ARBURG Practical Guide to Injection Moulding, Smithers Rapra, 2017.
[83] B.B. Kanbur, S. Suping, F. Duan, Design and optimization of conformal cooling channels for injection molding: a review, Int. J. Adv. Des. Manuf. Technol. 106 (7) (2020) 3253–3271, https://doi.org/10.1007/s00170-019-04697-9.
[84] Y. Xu, G. Liu, K. Dang, N. Fu, X. Jiao, J. Wang, P. Xie, W. Yang, A novel strategy to determine the optimal clamping force based on the clamping force change during injection molding, Polym. Eng. Sci. 61 (12) (2021) 3170–3178, https://doi.org/10.1002/pen.25829.
[85] V.-D. Le, V.-T. Hoang, Q.-B. Tao, L. Benabou, N.-H. Tran, D.-B. Luu, J.M. Park, Computational study on the clamping mechanism in the injection molding machine, Int. J. Adv. Des. Manuf. Technol. 121 (11) (2022) 7247–7261, https://doi.org/10.1007/s00170-022-09817-6.
[86] A.-G. Niculescu, C. Chircov, A.C. Bîrcă, A.M. Grumezescu, Fabrication and applications of microfluidic devices: a review, Int. J. Mol. Sci. 22 (4) (2021) 2011, https://doi.org/10.3390/ijms22042011.
[87] H. Zhang, H. Liu, N. Zhang, A review of microinjection moulding of polymeric micro devices, Micromachines 13 (9) (2022) 1530, https://doi.org/10.3390/mi13091530.
[88] G. Tosello, H.N. Hansen, Micro-injection-molding, Micro-Manufact. Eng. Technol. (2010) 90–113, https://doi.org/10.1016/B978-0-8155-1545-6.00006-5.
[89] U.M. Attia, S. Marson, J.R. Alcock, Micro-injection moulding of polymer microfluidic devices, Microfluid. Nanofluidics 7 (2009) 1–28, https://doi.org/10.1007/s10404-009-0421-x.
[90] J.B. Nielsen, R.L. Hanson, H.M. Almughamsi, C. Pang, T.R. Fish, A.T. Woolley, Microfluidics: innovations in materials and their fabrication and functionalization, Anal. Chem. 92 (1) (2019) 150–168, https://doi.org/10.1021/acs.analchem.9b04986.
[91] K. Ren, J. Zhou, H. Wu, Materials for microfluidic chip fabrication, Acc. Chem. Res. 46 (11) (2013) 2396–2406, https://doi.org/10.1021/ar300314s.
[92] R. Surace, G. Trotta, V. Bellantone, I. Fassi, The micro injection moulding process for polymeric components manufacturing. New technologies–trends, Innovations and Research, 2012, pp. 65–90, https://doi.org/10.5772/35299.
[93] S. Shi, L. Wang, Y. Pan, C. Liu, X. Liu, Y. Li, J. Zhang, G. Zheng, Z. Guo, Remarkably strengthened microinjection molded linear low-density polyethylene (LLDPE) via multi-walled carbon nanotubes derived nanohybrid shish-kebab structure, Compos. B Eng. 167 (2019) 362–369, https://doi.org/10.1016/j.compositesb.2019.03.007.
[94] F. Baruffi, M. Calaon, G. Tosello, Effects of micro-injection moulding process parameters on accuracy and precision of thermoplastic elastomer micro rings, Precis. Eng. 51 (2018) 353–361, https://doi.org/10.1016/j.precisioneng.2017.09.006.
[95] V. Piotter, K. Mueller, K. Plewa, R. Ruprecht, J. Hausselt, Performance and simulation of thermoplastic micro injection molding, Microsyst. Technol. 8 (2002) 387–390, https://doi.org/10.1007/s00542-002-0178-6.
[96] C. Hopmann, T. Fischer, New plasticising process for increased precision and reduced residence times in injection moulding of micro parts, CIRP J. Manuf. Sci. Technol. 9 (2015) 51–56, https://doi.org/10.1016/j.cirpj.2015.01.004.
[97] M. Calaon, F. Baruffi, G. Fantoni, I. Cirri, M. Santochi, H.N. Hansen, G. Tosello, Functional analysis validation of micro and conventional injection molding machines performances based on process precision and accuracy for micro manufacturing, Micromachines 11 (12) (2020) 1115, https://doi.org/10.3390/mi11121115.

[98] G. Fantoni, G. Tosello, D. Gabelloni, H.N. Hansen, Modelling injection moulding machines for micro manufacture applications through functional analysis, Proced. CIRP 2 (2012) 107–112, https://doi.org/10.1016/j.procir.2012.05.050.
[99] R. Surace, V. Basile, V. Bellantone, F. Modica, I. Fassi, Micro injection molding of thin cavities using stereolithography for mold fabrication, Polymers 13 (11) (2021) 1848, https://doi.org/10.3390/polym13111848.
[100] F. Baruffi, A. Charalambis, M. Calaon, R. Elsborg, G. Tosello, Comparison of micro and conventional injection moulding based on process precision and accuracy, Proced. CIRP 75 (2018) 149–154, https://doi.org/10.1016/j.procir.2018.04.046.
[101] M. Gülçür, E. Brown, T. Gough, B. Whiteside, Characterisation of microneedle replication and flow behaviour in ultrasonic micro-injection moulding through design of experiments, J. Manuf. Process. 102 (2023) 513–527, https://doi.org/10.1016/j.jmapro.2023.07.068.
[102] T. Evens, O. Malek, S. Castagne, D. Seveno, A. Van Bael, Controlling the geometry of laser ablated microneedle cavities in different mould materials and assessing the replication fidelity within polymer injection moulding, J. Manuf. Process. 62 (2021) 535–545, https://doi.org/10.1016/j.jmapro.2020.12.035.
[103] K.B. Mirza, C. Zuliani, B. Hou, F.S. Ng, N.S. Peters, C. Toumazou, Injection moulded microneedle sensor for real-time wireless pH monitoring, in: 2017 39th Annual International Conference of the IEEE Engineering in Medicine and Biology Society (EMBC), IEEE, 2017, https://doi.org/10.1109/EMBC.2017.8036794.
[104] R. Trichur, S. Kim, X. Zhu, J.W. Suk, C.-C. Hong, J.-W. Choi, C.H. Ahn, Development of plastic microneedles for transdermal interfacing using injection molding techniques, in: Micro Total Analysis Systems 2002: Proceedings of the Mtas 2002 Symposium, Held in Nara, Japan, vol. 1, Springer, 2002, https://doi.org/10.1007/978-94-010-0295-0_132, 3–7 November 2002.
[105] R.D. Boehm, J. Daniels, S. Stafslien, A. Nasir, J. Lefebvre, R.J. Narayan, Polyglycolic acid microneedles modified with inkjet-deposited antifungal coatings, Biointerphases 10 (1) (2015), https://doi.org/10.1116/1.4913378.
[106] W. Yu, J. Gu, Z. Li, S. Ruan, B. Chen, C. Shen, L.J. Lee, X. Wang, Study on the influence of microinjection molding processing parameters on replication quality of polylactic acid microneedle array product, Polymers 15 (5) (2023) 1199, https://doi.org/10.3390/polym15051199.
[107] L. Zhang, Y. Chen, J. Tan, S. Feng, Y. Xie, L. Li, Performance enhancement of PLA-based blend microneedle arrays through shish-kebab structuring strategy in microinjection molding, Polymers 15 (10) (2023) 2234, https://doi.org/10.3390/polym15102234.
[108] M. Gülçür, E. Brown, T. Gough, J.-M. Romano, P. Penchev, S. Dimov, B. Whiteside, Ultrasonic micromoulding: process characterisation using extensive in-line monitoring for micro-scaled products, J. Manuf. Process. 58 (2020) 289–301, https://doi.org/10.1016/j.jmapro.2020.08.033.
[109] T. Evens, S. Castagne, D. Seveno, A. Van Bael, Comparing the replication fidelity of solid microneedles using injection compression moulding and conventional injection moulding, Micromachines 13 (8) (2022) 1280, https://doi.org/10.3390/mi13081280.
[110] F. Sammoura, J. Kang, Y.-M. Heo, T. Jung, L. Lin, Polymeric microneedle fabrication using a microinjection molding technique, Microsyst. Technol. 13 (2007) 517–522, https://doi.org/10.1007/s00542-006-0204-1.
[111] F. Baruffi, M. Calaon, G. Tosello, Micro-injection moulding in-line quality assurance based on product and process fingerprints, Micromachines 9 (6) (2018) 293, https://doi.org/10.3390/mi9060293.
[112] S.H. Park, Y.-E. Yoo, W.I. Lee, Effect of a pressurized cavity on the replication of micro-patterns with injection molding, E-Polymers 16 (5) (2016) 373–378, https://doi.org/10.1515/epoly-2016-0061.
[113] S.-C. Nian, C.-Y. Wu, M.-S. Huang, Warpage control of thin-walled injection molding using local mold temperatures, ICHMT 61 (2015) 102–110, https://doi.org/10.1016/j.icheatmasstransfer.2014.12.008.
[114] K. Uchiumi, T. Takayama, H. Ito, A. Inou, Surface replication of molded products with microneedle features in injection molding, in: International Journal of Modern Physics: Conference Series, World Scientific, 2012, https://doi.org/10.1142/S2010194512003121.
[115] M. Calaon, G. Tosello, J. Garnaes, H. Hansen, Injection and injection-compression moulding replication capability for the production of polymer lab-on-a-chip with nano structures, JMiMi 27 (10) (2017) 105001, https://doi.org/10.1088/1361-6439/aa853f.
[116] S.J. Moon, S.S. Lee, H. Lee, T. Kwon, Fabrication of microneedle array using LIGA and hot embossing process, Microsyst. Technol. 11 (2005) 311–318, https://doi.org/10.1007/s00542-004-0446-8.
[117] R. Truckenmüller, P. Henzi, D. Herrmann, V. Saile, W. Schomburg, Bonding of polymer microstructures by UV irradiation and subsequent welding at low temperatures, Microsyst. Technol. 10 (2004) 372–374, https://doi.org/10.1007/s00542-004-0422-3.
[118] M. Sausse Lhernould, A. Delchambre, Innovative design of hollow polymeric microneedles for transdermal drug delivery, Microsyst. Technol. 17 (2011) 1675–1682, https://doi.org/10.1007/s00542-011-1355-2.
[119] P. Vanwersch, T. Evens, A. Van Bael, S. Castagne, Design, fabrication, and penetration assessment of polymeric hollow microneedles with different geometries, Int. J. Adv. Des. Manuf. Technol. (2024) 1–19, https://doi.org/10.1007/s00170-024-13344-x.
[120] K. Dong-Hak, K. Myung-Ho, Y. Chun, Development of a new injection molding technology: momentary mold surface heating process, J. Inject. Molding Technol. 5 (4) (2001) 229.
[121] C.-L. Xiao, H.-X. Huang, Development of a rapid thermal cycling molding with electric heating and water impingement cooling for injection molding applications, Appl. Therm. Eng. 73 (1) (2014) 712–722, https://doi.org/10.1016/j.applthermaleng.2014.08.027.
[122] M.-C. Jeng, S.-C. Chen, P.S. Minh, J.-A. Chang, C-s Chung, Rapid mold temperature control in injection molding by using steam heating, ICHMT 37 (9) (2010) 1295–1304, https://doi.org/10.1016/j.icheatmasstransfer.2010.07.012.
[123] P.C. Chang, S.J. Hwang, Experimental investigation of infrared rapid surface heating for injection molding, J. Appl. Polym. Sci. 102 (4) (2006) 3704–3713, https://doi.org/10.1002/app.24515.
[124] S. Gao, Z. Qiu, Z. Ma, Y. Yang, Development of high efficiency infrared-heating-assisted micro-injection molding for fabricating micro-needle array, Int. J. Adv. Des. Manuf. Technol. 92 (2017) 831–838, https://doi.org/10.1007/s00170-017-0169-5.
[125] U. Heredia-Rivera, I. Ferrer, E. Vázquez, Ultrasonic molding technology: recent advances and potential applications in the medical industry, Polymers 11 (4) (2019) 667, https://doi.org/10.3390/polym11040667.
[126] S. Gao, Z. Qiu, J. Ouyang, The improvement effect and mechanism of longitudinal ultrasonic vibration on the injection molding quality of a polymeric micro-needle array, Polymers 11 (1) (2019) 151, https://doi.org/10.3390/polym11010151.
[127] K.L. Yung, Y. Xu, C. Kang, H. Liu, K. Tam, S. Ko, F. Kwan, T.M. Lee, Sharp tipped plastic hollow microneedle array by microinjection moulding, JMiMi 22 (1) (2011) 015016, https://doi.org/10.1088/0960-1317/22/1/015016.
[128] C.T. Uppuluri, J. Devineni, T. Han, A. Nayak, K.J. Nair, B.R. Whiteside, D.B. Das, B.N. Nalluri, Microneedle-assisted transdermal delivery of Zolmitriptan: effect of microneedle geometry, in vitro permeation experiments, scaling analyses and numerical simulations, Drug Dev. Ind. Pharm. 43 (8) (2017) 1292–1303, https://doi.org/10.1080/03639045.2017.1313862.
[129] P. Vanwersch, T. Evens, O. Malek, A. Van Bael, S. Castagne, Fs laser ablation and injection molding simulations for the manufacturing of polymer hollow microneedles, Int. J. Adv. Des. Manuf. Technol. (2025) 1–17, https://doi.org/10.1007/s00170-025-15148-z.
[130] M.J. Kim, S.C. Park, B. Rizal, G. Guanes, S.-K. Baek, J.-H. Park, A.R. Betz, S.-O. Choi, Fabrication of circular obelisk-type multilayer microneedles using micro-milling and spray deposition, Front. Bioeng. Biotechnol. 6 (2018) 54, https://doi.org/10.3389/fbioe.2018.00054.
[131] D.M. Wirth, L.G. McCline, J.K. Pokorski, Fabrication of an inexpensive injection molding instrument for rapid prototyping of high precision parts, Polymer 264 (2023) 125521, https://doi.org/10.1016/j.polymer.2022.125521.
[132] R.E. Lutton, E. Larrañeta, M.-C. Kearney, P. Boyd, A.D. Woolfson, R.F. Donnelly, A novel scalable manufacturing process for the production of hydrogel-forming microneedle arrays, Int. J. Pharm. 494 (1) (2015) 417–429, https://doi.org/10.1016/j.ijpharm.2015.08.049.
[133] Y. Sato, M. Tsukamoto, T. Nariyama, K. Nakai, F. Matsuoka, K. Takahashi, S. Masuno, T. Ohkubo, H. Nakano, Analysis of laser ablation dynamics of CFRP in order to reduce heat affected zone, in: Laser Applications in Microelectronic and Optoelectronic Manufacturing (LAMOM) XIX, 2014, https://doi.org/10.1117/12.2040288. SPIE.
[134] M. Zaied, I. Miraoui, M. Boujelbene, E. Bayraktar, Analysis of heat affected zone obtained by CO2 laser cutting of low carbon steel (S235), in: AIP Conf. Proc., American Institute of Physics, 2013, https://doi.org/10.1063/1.4849285.
[135] H. Izumi, M. Suzuki, S. Aoyagi, T. Kanzaki, Realistic imitation of mosquito's proboscis: electrochemically etched sharp and jagged needles and their cooperative inserting motion, Sensor Actuator Phys. 165 (1) (2011) 115–123, https://doi.org/10.1016/j.sna.2010.02.010.
[136] J. Wang, C. Hopmann, C. Kahve, T. Hohlweck, J. Alms, Measurement of specific volume of polymers under simulated injection molding processes, Mater. Des. 196 (2020) 109136, https://doi.org/10.1016/j.matdes.2020.109136.
[137] C. Rytka, N. Opara, N.K. Andersen, P.M. Kristiansen, A. Neyer, On the role of wetting, structure width, and flow characteristics in polymer replication on micro-and nanoscale, Macromol. Mater. Eng. 301 (5) (2016) 597–609, https://doi.org/10.1002/mame.201500350.
[138] J. Vera, E. Contraires, A.-C. Brulez, M. Larochette, S. Valette, S. Benayoun, Wetting of polymer melts on coated and uncoated steel surfaces, Appl. Surf. Sci. 410 (2017) 87–98, https://doi.org/10.1016/j.apsusc.2017.02.067.
[139] G. Trotta, B. Stampone, I. Fassi, L. Tricarico, Study of rheological behaviour of polymer melt in micro injection moulding with a miniaturized parallel plate rheometer, Polym. Test. 96 (2021) 107068, https://doi.org/10.1016/j.polymertesting.2021.107068.
[140] G. Yilmaz, T. Ellingham, L.S. Turng, Injection and injection compression molding of ultra-high-molecular weight polyethylene powder, Polym. Eng. Sci. 59 (s2) (2019) E170–E179, https://doi.org/10.1002/pen.25020.
[141] J. Mewis, N.J. Wagner, Thixotropy, Adv. Colloid Interface Sci. 147 (2009) 214–227, https://doi.org/10.1016/j.cis.2008.09.005.
[142] J. Mewis, Thixotropy-a general review, J. Non-Newtonian Fluid Mech. 6 (1) (1979) 1–20, https://doi.org/10.1016/0377-0257(79)87001-9.
[143] G. Trotta, S. Cacace, Q. Semeraro, Optimizing process parameters in micro injection moulding considering the part weight and probability of flash formation, J. Manuf. Process. 79 (2022) 250–258, https://doi.org/10.1016/j.jmapro.2022.04.048.
[144] M. Mani, R. Surace, P. Ferreira, J. Segal, I. Fassi, S. Ratchev, Process parameter effects on dimensional accuracy of micro-injection moulded part, J. Micro Nano-Manufact. 1 (3) (2013) 031003, https://doi.org/10.1115/1.4025073.
[145] B. Sha, S. Dimov, C. Griffiths, M. Packianather, Investigation of micro-injection moulding: factors affecting the replication quality, J. Mater. Process. Technol. 183 (2–3) (2007) 284–296, https://doi.org/10.1016/j.jmatprotec.2006.10.019.
[146] H. Zhang, F. Fang, M.D. Gilchrist, N. Zhang, Filling of high aspect ratio micro features of a microfluidic flow cytometer chip using micro injection moulding, JMiMi 28 (7) (2018) 075005, https://doi.org/10.1088/1361-6439/aab7bf.

[147] F. Baruffi, M. Gülçür, M. Calaon, J.-M. Romano, P. Penchev, S. Dimov, B. Whiteside, G. Tosello, Correlating nano-scale surface replication accuracy and cavity temperature in micro-injection moulding using in-line process control and high-speed thermal imaging, J. Manuf. Process. 47 (2019) 367–381, https://doi.org/10.1016/j.jmapro.2019.08.017.
[148] K.A. Stelson, Calculating cooling times for polymer injection moulding, Proc. Inst. Mech. Eng. Pt. B: J. Eng. Manuf. 217 (5) (2003) 709–713, https://doi.org/10.1243/095440503322011443.
[149] C. Plamadeala, S.R. Gosain, F. Hischen, B. Buchroithner, S. Puthukodan, J. Jacak, A. Bocchino, D. Whelan, C. O'Mahony, W. Baumgartner, Bio-inspired microneedle design for efficient drug/vaccine coating, Biomed. Microdevices 22 (2020) 1–9, https://doi.org/10.1007/s10544-019-0456-z.
[150] L.K. Vora, R.F. Donnelly, E. Larrañeta, P. González-Vázquez, R.R.S. Thakur, P. R. Vavia, Novel bilayer dissolving microneedle arrays with concentrated PLGA nano-microparticles for targeted intradermal delivery: proof of concept, J. Contr. Release 265 (2017) 93–101, https://doi.org/10.1016/j.jconrel.2017.10.005.
[151] G. Tosello, M. Gulcur, B. Whiteside, P. Coates, A. Luca, P. Vinícius, O. Riemer, I. Danilov, M.Y. Zanjani, M. Hackert-Oschätzchen, Micro product and process fingerprints for zero-defect net-shape micromanufacturing, in: Proceedings of the 19th International Conference and Exhibition (EUSPEN 2019), The European Society for Precision Engineering and Nanotechnology, 2019.
[152] J. Wang, Q. Mao, N. Jiang, J. Chen, Effects of injection molding parameters on properties of insert-injection molded polypropylene single-polymer composites, Polymers 14 (1) (2021) 23, https://doi.org/10.3390/polym14010023.
[153] C. Yang, X.-H. Yin, G.-M. Cheng, Microinjection molding of microsystem components: new aspects in improving performance, JMiMi 23 (9) (2013) 093001, https://doi.org/10.1088/0960-1317/23/9/093001.
[154] K. Maghsoudi, R. Jafari, G. Momen, M. Farzaneh, Micro-nanostructured polymer surfaces using injection molding: a review, Mater. Today Commun. 13 (2017) 126–143, https://doi.org/10.1016/j.mtcomm.2017.09.013.
[155] C. Griffiths, G. Tosello, S. Dimov, S. Scholz, A. Rees, B. Whiteside, Characterisation of demoulding parameters in micro-injection moulding, Microsyst. Technol. 21 (2015) 1677–1690, https://doi.org/10.1007/s00542-014-2269-6.
[156] S. Zaki, N. Zhang, M.D. Gilchrist, Microscale shaping and rounding of ridge arrays and star pattern features on nickel mould via electrochemical polishing, Adv. Manufact. (2024) 1–20, https://doi.org/10.1007/s40436-023-00474-w.
[157] M. Packianather, C. Griffiths, W. Kadir, Micro injection moulding process parameter tuning, Proced. CIRP 33 (2015) 400–405, https://doi.org/10.1016/j.procir.2015.06.093.
[158] M. Babenko, J. Sweeney, P. Petkov, F. Lacan, S. Bigot, B. Whiteside, Evaluation of heat transfer at the cavity-polymer interface in microinjection moulding based on experimental and simulation study, Appl. Therm. Eng. 130 (2018) 865–876, https://doi.org/10.1016/j.applthermaleng.2017.11.022.
[159] V. Bellantone, R. Surace, G. Trotta, I. Fassi, Replication capability of micro injection moulding process for polymeric parts manufacturing, Int. J. Adv. Manuf. Technol. 67 (2013) 1407–1421, https://doi.org/10.1007/s00170-012-4577-2.
[160] Q. Nguyen, X. Chen, Y. Lam, C. Yue, Effects of polymer melt compressibility on mold filling in micro-injection molding, JMiMi 21 (9) (2011) 095019, https://doi.org/10.1088/0960-1317/21/9/095019.
[161] M. Sorgato, M. Babenko, G. Lucchetta, B. Whiteside, Investigation of the influence of vacuum venting on mould surface temperature in micro injection moulding, Int. J. Adv. Des. Manuf. Technol. 88 (2017) 547–555, https://doi.org/10.1007/s00170-016-8789-8.
[162] V. Ebrahiminejad, Z. Faraji Rad, Design, development, and testing of polymeric microblades: a novel design of microneedles for biomedical applications, Adv. Mater. Interfac. 9 (2022) 2201115, https://doi.org/10.1002/admi.202201115.
[163] V. Ebrahiminejad, A. Malek-Khatabi, Z. Faraji Rad, Influence of low-frequency vibration and skin strain on insertion mechanics and drug diffusion of PVA/PVP dissolving microneedles, Adv. Mater. Technol. 9 (2024) 2301272, https://doi.org/10.1002/admt.202301272.

Pouria Azarikhah completed his B.Sc. in Mechanical Engineering at K. N. Toosi University of Technology, Iran (2014), followed by an M.Sc. in Mechanical Engineering at Iran University of Science and Technology in 2017. He is currently pursuing a Ph.D. at the University of Southern Queensland under the supervision of Dr. Zahra Faraji Rad. His research focuses on manufacturing polymeric microneedles using injection moulding techniques with novel thermoplastic materials, emphasising a mass production approach.

Asim Mushtaq is a Senior Research Technical Officer at the Centre for Future Materials, University of Southern Queensland. He received his PhD from the School of Chemistry and Molecular Biosciences at the University of Queensland in 2022. His current research interests include chemical modification of polymers, nano-drug delivery, microneedles for point-of-care diagnostics and agriculture applications.

Khaled Mohammed Saifullah obtained his PhD in Biomedical Engineering from the University of Southern Queensland (UniSQ). He also holds a BSc in Electrical and Electronic Engineering from the American International University-Bangladesh (AIUB) and an MEngSc in Electrical Engineering from the University of New South Wales (UNSW), Australia. His research focuses on developing microneedle integrated wearable sensors for the detection of biomarkers in interstitial fluid (ISF). He currently works as an In Vivo Biomedical Engineer at Hazelton Technologies Pty Ltd, developing microneedle-based wearable biosensors.

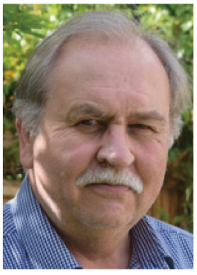

Philip D. Prewett is an Emeritus Professor of Nanotechnology at Birmingham University, UK, having previously held the Lucas Chair in Mechanical Engineering until 2011. He was previously Head of R&D and Individual Merit Scientist at the Central Microstructure Facility, Rutherford Appleton Laboratory. He gained a BSc with 1st Class Honors in Physic from University College of Wales Swansea and a DPhil in Plasma Science from Oxford University. He is a Fellow of the Institute of Physics and a Fellow of the Learned Society of Wales. He works in the industry and academia and is the founder and director of four start-up technology companies.

Graham J. Davies is the former Dean of Engineering at the University of New South Wales, Sydney, Australia. He graduated from the University of Wales, UK, and he holds the highest degree of DSc. He has held senior posts in academia at the University of Birmingham and as Director in charge of British Telecom's Corporate Research Programme. He is an Emeritus Professor at both UNSW and the University of Birmingham. His research interests are in the fields of bio-MEMS and the growth of III–V semiconductors by MBE. He is a Fellow of the Royal Academy of Engineering and the Learned Society of Wales.

Zahra Faraji Rad is an associate professor of mechanical engineering at the University of the Sunshine Coast. She received a MEng with 1st Class Honors in biomedical engineering from the University of Birmingham (2010). She obtained her Ph.D. from the Universities of New South Wales and Birmingham as the first joint Ph.D. candidate from the two universities under the international Universitas 21 partnership (2016). Her current research interests include microneedles for point-of-care diagnostics and drug delivery. She is the recipient of the 2021 Science and Innovation Awards for Young People in Agriculture, Fisheries and Forestry in the CSIRO Biosecurity Digital Innovation Award category.